RESEARCH LABORATORIES FOR THE ENGINEERING SCIENCES

SCHOOL OF ENGINEERING AND APPLIED SCIENCE

UNIVERSITY OF VIRGINIA

Charlottesville, Virginia 22901

Annual Report

OPTIMIZATION OF MLS RECEIVERS FOR MULTIPATH ENVIRONMENTS

NASA Grant NSG 1128

Submitted to:

NASA Scientific & Technical Information Facility
PO Box 8757
Baltimore/Washington International Airport
Baltimore, MD 21240

Submitted by:

G. A. McAlpine
J. H. Highfill III
C.-P. J. Tzeng
Ghassem Koleyni

Report No. UVA/528062/EE78/106

October 1978

RESEARCH LABORATORIES FOR THE ENGINEERING SCIENCES

Members of the faculty who teach at the undergraduate and graduate levels and a number of professional engineers and scientists whose primary activity is research generate and conduct the investigations that make up the school's research program. The School of Engineering and Applied Science of the University of Virginia believes that research goes hand in hand with teaching. Early in the development of its graduate training program, the School recognized that men and women engaged in research should be as free as possible of the administrative duties involved in sponsored research. In 1959, therefore, the Research Laboratories for the Engineering Sciences (RLES) was established and assigned the administrative responsibility for such research within the School.

The director of RLES—himself a faculty member and researcher—maintains familiarity with the support requirements of the research under way. He is aided by an Academic Advisory Committee made up of a faculty representative from each academic department of the School. This Committee serves to inform RLES of the needs and perspectives of the research program.

In addition to administrative support, RLES is charged with providing certain technical assistance. Because it is not practical for each department to become self-sufficient in all phases of the supporting technology essential to present-day research, RLES makes services available through the following support groups: Machine Shop, Instrumentation, Facilities Services, Publications (including photographic facilities), and Computer Terminal Maintenance.

Annual Report

OPTIMIZATION OF MLS RECEIVERS FOR MULTIPATH ENVIRONMENTS

NASA Grant NSG 1128

Submitted to:

NASA Scientific & Technical Information Facility
PO Box 8757
Baltimore/Washington International Airport
Baltimore, MD 21240

Submitted by:

G. A. McAlpine
J. H. Highfill III
C.-P. J. Tzeng
Ghassem Koleyni

Department of Electrical Engineering
Research Laboratories for the Engineering Sciences
School of Engineering and Applied Science
UNIVERSITY OF VIRGINIA
Charlottesville, Virginia

Report No. UVA/528062/EE78/106
October 1978

Copy No. 2

TABLE OF CONTENTS

TABLE OF CONTENTS (continued)

LIST OF FIGURES

LIST OF FIGURES (continued)

LIST OF TABLES

CHAPTER 1

INTRODUCTION

This work is part of the project, "Microwave Landing System " (MLS), undertaken by the Communication Systems Laboratory, Department of Electrical Engineering, University of Virginia, under Grant NSG 1128. Current work in progress is concerned with the reduced-order receiver (suboptimal receiver) analysis in multipath environments. In this chapter the origin and objective of MLS will be described briefly. Chapter 2 and Chapter 3 will be the review of signal modeling in MLS, the optimum receiver structure, and its performance. Readers are requested to refer to the prior reports submitted by the Communication Systems Laboratory [1-4]. Chapter 4 will be a summary of the derivation of the suboptimal receiver. Chapter 5 is the description of a computer-oriented technique which we used in the simulation study of the suboptimal receiver. Chapters 6 and 7 present the results and conclusion obtained from the research for the suboptimal receiver.

Background

Since man learned how to fly, there has existed a need for a landing guidance system to aid the pilot during periods of restricted visibility. The Instrument Landing System (ILS), which was adopted by the International Civil Aviation Organization (ICAO) in 1949, is presently the international standard. The limitation to ILS, such as

susceptability to interference and weather degradation. shortage of frequency channels, large size of antennas, and the restriction to one narrow approach path has raised the need of a new universal approach and landing system. In 1970 the Radio Technical Commission for Aeronautics recommended the development of a universal microwave landing system in 1971. At this time, the United States selected the Time Reference Scanning Beam (TRSB) as its choice for the ICAO program.

In this report MLS will be referred to as the MLS System, i.e. TRSB system which has been selected by the United States.

Objectives

The Microwave Landing System provides an electronic guidance in an air terminal area for an approaching aircraft to compute its position in space relative to a fixed ground reference. The required information is derived by the aircraft's receiver from ground-transmitted microwave signals. The goal of the project is to develop an aircraft receiver which can give optimal performance in the multipath environments found in air terminal areas.

CHAPTER 2

STATE-SPACE APPROACH

State-space approach is the focus of modern control theory. Several factors influence the development of modern control theory:

a. The necessity of dealing with a more realistic model of the system.

b. The shift in emphasis towards optimal control and optimal system design.

c. The continuing developments in digital computer technology.

d. The shortcomings of previous approaches.

State variables consist of a minimum set of variables which are essential for completely describing the internal status, i.e. state of the system. Conventional input-output equations, or the transfer functions for linear systems, do not give us any information about the internal properties of the system. Optimal control makes it even more difficult to avoid dealing with unsatisfactory nonlinearities, which are very difficult to represent in conventional input-output equations. The development of modern digital computers makes possible the solution of problems which were previously insolvable. Since computers work in the time domain, it is more efficient for a computer to directly integrate differential equations than to use transform-inverse transformation

methods that were usually used in conventional control systems. These factors thus justify the use of the state-space approach of modern control theory -- particularly, as it applies to MLS.

Signal Modeling

The whole system is modeled by the state-space approach. The angular coordinate [1] to be estimated and other relevant quantities that evolve are assembled into an N-dimensional state vector modeled as the solution of a suitable linear difference equation evolving in discrete time, from scan to scan, and excited by a white zero-mean random process, $\{Z(k), k = 0, 1, \ldots\}$.

$$x \triangleq (\alpha, \theta, \dot{\theta}, \alpha_R, \theta_R, \dot{\theta}_R, \beta, \omega_{sc})^T \tag{2.1}$$

where $(\ )^T$ denotes transpose and $(\dot{})$ denotes $\frac{d(\ )}{dt}$ and

$$\alpha = \alpha(k) = \text{direct path signal-to-noise ratio (SNR)} \tag{2.2}$$

$$\theta = \theta(k) = \text{angular coordinate of own A/C} \tag{2.3}$$

$$\alpha_R = \alpha_R(k) = \text{multipath SNR} \tag{2.4}$$

$$\theta_R = \theta_R(k) = \text{angular coordinate of reflector specular point} \tag{2.5}$$

$$\beta = \beta(k) = \text{direct-path to multipath phase difference at the beginning of the scan} \tag{2.6}$$

$$\beta(k+1) = \beta(k) + \omega_{sc} \cdot T_k \tag{2.7}$$

where T_k = time interval

$$\omega_{sc} = \text{the scalloping rate} \tag{2.8}$$

The system difference equation can be expressed as

$$x(K+1) = F(K)\,x(K) + G(K)\,z(K)$$
$$u(K) = h(x(K), n(K)) \tag{2.9}$$

where u(k) is the observation, n(k) is receiver noise.

The j^{th} component of u, u_j, can be expressed more specifically as

$$u_j = \left\{\alpha\, p[\theta - \theta_A(\tau_j)] + \alpha_R\, p[\theta_R - \theta_A(\tau_j)]\cos(\beta + \omega_{sc}\tau_j) + n_{cj}\right\}^2 + \left\{\alpha_R\, p[\theta_R - \theta_A(\tau_j)]\sin(\beta + \omega_{sc}\tau_j) + n_{sj}\right\}^2 \tag{2.10}$$

in terms of a discrete-time variable, τ_j, local to the scan and, assuming the presence of a direct-path component, a single multipath component and receiver noise where

$\theta_A(\cdot)$ = the transmitting antenna-scanning function (2.11)

$p[\cdot]$ = the transmitting antenna selectivity function (2.12)

and

n_{cj}, n_{sj} = independent Gaussian random variables with mean-zero variance 0.5 (2.13)

CHAPTER 3

THE OPTIMAL RECEIVER

This chapter contains the summary of the optimal receiver structure, operation, and performance. Readers are referred to [2] for details. Theory and results in this chapter were used in the next chapter for the derivation of the suboptimal receiver.

Receiver Structure

The objective of the desired MLS angle receiver is to produce an estimate of the A/C angular coordinate, θ, which is minimally affected by multipath interference. Recursive state estimation was used in the receiver system. If we define

$$U(K) \triangleq \{u(k),\ k = 0, 1, \ldots K\} \quad = \text{the sequence of observations from some initial time through the present,} \tag{3.1}$$

and

$$\hat{x}(K|K) \quad \triangleq \text{estimate of } x(k), \text{ given } U(k) \tag{3.2}$$

then the estimation evolution is described as follows.

$$\hat{x}(K+1) \triangleq \hat{x}(K|K-1) + \xi(K|K) \tag{3.3}$$

where

$$\hat{x}(k|k-1) \triangleq F(k-1)\,\hat{x}(k-1|k-1) \tag{3.4}$$

$\xi(k|k)$ = estimate of the error in $\hat{x}(k|k-1)$, given $U(k)$. (3.5)

This is complicated to compute. In our research we assume ξ is small in some sense and use the following equation with good results.

$$\xi(k|k) = K(k)\,\epsilon(k|k) \tag{3.6}$$

where

$\epsilon(k|k) \triangleq$ estimate of the error in $\hat{x}(k|k-1)$ in the neighborhood of zero error, given u(k); (3.7)

$K(k) \triangleq$ a gain matrix, depending on $\hat{x}(k|k-1)$, $Q(k)$, and statistics of $\epsilon(k|k)$, (3.8)

$$Q(k) \triangleq \langle z(k)\,z^{T}(k) \rangle = \mathrm{Diag}\,(Q_{11}, Q_{22}, Q_{33}, Q_{44}, Q_{55}) \tag{3.9}$$

(Diag. means Diagonal)

The calculation of $\epsilon(k|k)$ is based on the Locally Optimum Estimation (LOE) criterion of Murphy [5]. LOE, as well as the recursive estimation Kalman filter, constitutes the following structure of our receiver.

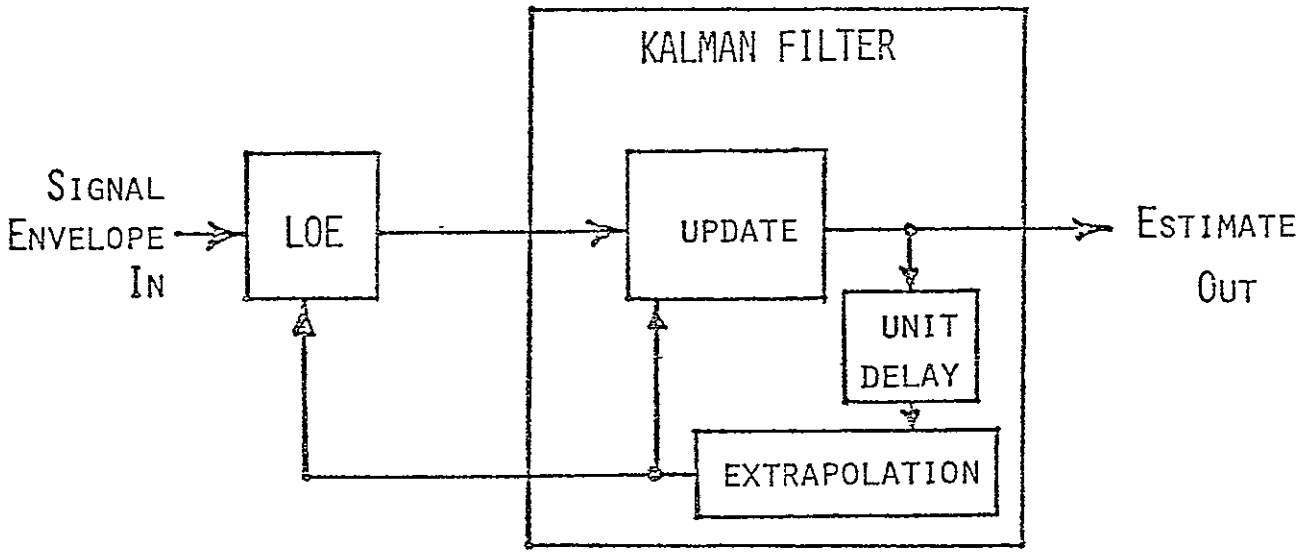

Fig. 3.1

As shown in Fig. 3.1, a Locally Optimum Estimator (LOE) used the last estimate and extracts all usable information from the new scan data. A Kalman filter integrates the output of the LOE with the past to produce an optimal estimate, given all data through the present.

Generally, the Kalman filter uses the following formulas recursively to achieve the optimum estimate.

$$\hat{x}(K|K-1) = F(K-1)\hat{x}(K-1|K-1) \tag{3.10}$$

$$P(K|K-1) = F(K-1)P(K-1|K-1)F^{T}(K-1) + G(K-1)Q(K-1)G^{T}(K-1) \tag{3.11}$$

$$K(K) = P(K|K-1)H^{T}\left[HP(K|K-1)H^{T} + R(K)\right]^{-1} \tag{3.12}$$

$$\hat{x}(K|K) = \hat{x}(K|K-1) + K(K)\left[\hat{z}(K|K) - H\hat{x}(K|K-1)\right] \tag{3.13}$$

$$P(K|K) = P(K|K-1) - K(K)\,HP(K|K-1) \tag{3.14}$$

$$= [I - K(K)H]\,P(K|K-1)\,[I - K(K)H]^T + K(K)\,R(K)\,K^T(K) \tag{3.15}$$

where $\hat{\hat{\gamma}}$ is a "pre-estimate" of parameter vector γ using the LOE, $\hat{e}$, as follows:

$$\hat{\hat{Y}}(K|K) = \hat{Y}(K|K-1) + \hat{e}(K) \tag{3.16}$$

$$= H\hat{\gamma}(K|K-1) + \hat{e}(K) \tag{3.17}$$

G is as defined in prior work [2].

$$\hat{\gamma} = [Y(K) - \hat{e}(K)] - \hat{e}(K) \tag{3.18}$$

$$= Hx(K) + v(K) \tag{3.19}$$

where

$$H \triangleq \text{masking matrix associated with the choice of } Y \tag{3.20}$$

and, finally, the LOE estimation error is

$$v(K) \triangleq \hat{e}(K) - e(K) \tag{3.21}$$

Following Murphy's concept [5] in LOE, assuming locally optimum estimation, and using LOE pre-estimate, $\hat{\hat{Y}}$, we could simplify the algorithm of the Kalman filter. Equation (3.13) could be rewritten as [2]

$$\hat{X}(k|k) = \hat{x}(k|k-1) + M(k)\,\Lambda\left(u \,\middle|\, \hat{q}_0\right) \tag{3.22}$$

where

$$M(K) = P(K|K-1)\,H^T\left[I + \Xi\, HPH^T\right]^{-1} \tag{3.23}$$

and $\Lambda(u|\hat{\gamma})$ is a vector with i^{th} component, as follows:

$$\Lambda_i(u|\hat{\gamma}) = \begin{cases} \left\{ \frac{\partial}{\partial \gamma_i} \ln \lambda(u|\gamma(\gamma) \right., & \text{if } \lambda \neq 0 \\ 0 \quad , & \text{otherwise} \end{cases} \tag{3.24}$$

in which $\lambda(u|\gamma)$ is the likelihood ration [3] and

$$\Phi = \langle \Lambda \Lambda^T \mid \text{NO ERROR IN } \hat{\gamma} \rangle \tag{3.25}$$

(3.14) could also be written as

$$P(K|K) = \left[I - M\Xi H\right] P(K|K-1) \left[I - M\Xi H\right]^T + M\Xi M^T \tag{3.26}$$

LOE, Ξ, and Λ

The concept and development of LOE was expounded by Murphy [5] in 1968 and summarized in [1] and applied to the A/C angular coordinate estimate problem in MLS.

The LOE first assembled a selected subset of the state vector into a parameter vector γ and then processed the observations u to obtain an estimate e of the error in the current γ - estimate.

$$\hat{e} \triangleq \Xi^{-1} \Lambda(u|\hat{\gamma}) \tag{3.27}$$

where

$$\Xi \triangleq \langle \Lambda(u|\hat{\gamma}) \Lambda^T(u|\hat{\gamma}) \mid \text{NO ERRORS IN } \hat{\gamma} \rangle \tag{3.28}$$

$$\hat{q} \triangleq q(r)\Big|_{r=\hat{r}} \tag{3.29}$$

$$q_j(r) = u_j\Big|_{n_g = n_{sj} = 0}, \text{ where } u_j \text{ is given by (2.10)} \tag{3.30}$$

where

$$\Lambda(u|\hat{q}) = \left[\frac{\partial}{\partial r}\hat{L}\cdot\lambda(u|q(r)\right]_{r=\hat{r}}, \text{ as above} \tag{3.31}$$

$$\text{where} \quad r = (d, \theta, \sigma_R, b_R, \beta)^T \tag{3.32}$$

and $\lambda(u_j)$ is the likelihood ratio, as follows, for J samples/scan:

$$\lambda(u|q) = \prod_{j=1}^{J}\lambda_j = \prod_{j=1}^{J}\left[I_0(2\sqrt{a_{sj}u_j})\exp(-a_{bj})\right], \tag{3.32a}$$

and $I_0(\,)$ is the modified Bessel function of the first kind, zeroth order.

Following [2], we can write

$$\Lambda = Dw \tag{3.33}$$

$$\Sigma = DHwD^T \tag{3.34}$$

where

$$D \triangleq \left(\frac{\partial\lambda_1}{\partial r} \quad \frac{\partial\lambda_2}{\partial r} \quad \cdots \quad \frac{\partial\lambda_J}{\partial r}\right), \quad \text{a MATRIX} \tag{3.35}$$

$$W(u|\hat{q}) = \begin{pmatrix} \vdots \\ 4u_j \frac{M_1}{M_0}(+\hat{q}_i u_j) - 1 \\ \vdots \end{pmatrix}, \text{ a } J \text{ vector} \tag{3.36}$$

in which

$$M_1(z) = \frac{d}{dz} M_0(z) \tag{3.37}$$

$$M_0(z^j) \triangleq I_0(z) \tag{3.38}$$

and

$$H_W(\hat{q}_j) \triangleq \langle W(u|\hat{q}_j) W^T(u|\hat{q}_j) \mid \hat{q}_i \text{ is without error} \rangle \tag{3.39}$$

$$= \text{Diag}\{h_1(\hat{q}_i), h_2(\hat{q}_i), \cdots h_J(\hat{q}_i)\} \tag{3.40}$$

where

$$h_j(\hat{q}_i) \triangleq \langle W_j^2(u;\hat{q}_i) \mid \hat{q}_i \text{ is without error} \rangle \tag{3.41}$$

$$\approx \frac{1}{1 + z\hat{q}_{ij}} \quad (\text{see ref. [2]}) \tag{3.42}$$

An approximation for the j^{th} component of $w(u|q)$ in (3.36), above, was described in [4], as follows:

$$W_j(u|\theta) = \frac{u_j}{\sqrt{1 + \sum_{k=1}^{n} u_k^2}} - 1 \qquad (3.43)$$

CHAPTER 4

INTRODUCTION TO THE SUBOPTIMAL RECEIVER

The optimal receiver generally outperformed the threshold receiver at the expense of complexity. Five parameters, α, θ, α_R, θ_R, and β, had to be acquired before the multipath signal could be tracked in the Kalman filter and LOE system. The difficulty in acquiring β has, in fact, prevented the application of the optimal receiver. Consequently, we designed a reduced-order receiver, also called the suboptimal receiver, which resolved this difficulty while simplifying the receiver structure.

Derivation of the Suboptimal Receiver

In the optimal receiver the likelihood ratio, λ, involving the quantities $\mathcal{A}$ and $\underline{z}$, was used for the LOE system. In the suboptimal receiver we were concerned with a likelihood ratio obtained by averaging $\underline{\beta}$ out of λ. The parameter vector estimate, Υ, became a four-dimensional vector

$$\Upsilon = (\alpha, \theta, \alpha_R, \theta_R)^T \qquad (4.1)$$

Following the derivations in [5], the likelihood ratio, $\overline{\lambda}$, in which β is averaged out, can be written as

$$\overline{\lambda}(\Upsilon, u) \triangleq \prod_{j=1}^{J} \overline{\lambda}_j(\Upsilon, u) \qquad (4.2)$$

$$\bar{\lambda}_j(\gamma, u) = \frac{1}{\pi}\int_0^{\pi} \lambda_j(\gamma, u_j, \beta_j)\, d\beta_j \tag{4.3}$$

The structure of the suboptimal receiver is similar to that of the optimal receiver, except for the following:

1. The dimension of the state vector of LOE and Kalman filter are less in the suboptimal receiver.
2. The computation of Λ and $\underline{\Phi}$, which were used in LOE, are different, since $\bar{\lambda}$ is a function averaged over β.

Formulas for the computing of Λ and $\underline{\Phi}$ were in [5] and are summarized in the following:

$$\Lambda_j = \frac{\frac{\partial}{\partial \gamma}\bar{\lambda}_j}{\bar{\lambda}_j} = \frac{\int_0^{\pi} \frac{\partial}{\partial \gamma}\lambda_j(\gamma, u_j, \beta_j)\, d\beta_j}{\int_0^{\pi} \lambda_j(\gamma, u_j, \beta_j)\, d\beta_j} \tag{4.4}$$

$$= \frac{\int_0^{\pi} \frac{\partial q_{ij}}{\partial \gamma}\frac{\partial \lambda_j}{\partial q_{ij}}\, d\beta_j}{\int_0^{\pi} \lambda_j\, d\beta_j} \tag{4.5}$$

where λ_j is defined in (3.32a)

$$q_{ij} \triangleq \alpha_j^2 \rho_j^2(0) + 2\alpha\alpha_R \rho_j(\theta)\rho_j(\beta_R)\cos\beta_j + \alpha_R^2 \rho_j^2(\theta_R) = q_{ij}(\gamma) \tag{4.6}$$

If we define

$$q_{ij} \triangleq q_{Aij} + q_{Bij}\cos\beta_j \tag{4.7}$$

or

$$q_j = q_{Aj}\,(1 + B_j \cos\beta_j) \tag{4.8}$$

where

$$q_{Aj} = \alpha^2 p_j(\theta) + \alpha_R^2 \beta_j^2(\theta_R) \qquad (q_{Aj} \geq 0) \tag{4.9}$$

$$q_{Bj} = 2\alpha\alpha_R \beta_j(\theta)\,\beta_j(\theta_R) \qquad (-q_{Aj} \leq q_{Bj} \leq q_{Aj}) \tag{4.10}$$

$$B_j = \frac{q_{Bj}}{q_{Aj}} \quad \text{if } q_{Aj} \neq 0 \qquad (|B_j| \leq 1) \tag{4.11}$$

Then, λ_j can be written as

$$\lambda_j = \frac{\partial q_{Aj}}{\partial x}\,\frac{\int_0^\pi \frac{\partial \lambda_j}{\partial q_{Aj}}\,d\beta_j}{\int_0^\pi \lambda_j\,d\beta_j} + \frac{\partial q_{Bj}}{\partial x}\,\frac{\int_0^\pi \frac{\partial \lambda_j}{\partial q_{Bj}}\cos\beta_j\,d\beta_j}{\int_0^\pi \lambda_j\,d\beta_j} \tag{4.12}$$

So, we can then write

$$\lambda \triangleq \lambda_A + \lambda_B = D_A W_A + D_B W_B \tag{4.13}$$

where

$$D_A = \begin{pmatrix} \cdots & \frac{\partial}{\partial x_1} q_{Aj} & \cdots \\ & \vdots & \\ \cdots & \frac{\partial}{\partial x_n} q_{Aj} & \cdots \end{pmatrix}, \qquad D_B = \begin{pmatrix} \cdots & \frac{\partial}{\partial x_1} F_j & \cdots \\ & \vdots & \\ \cdots & \frac{\partial}{\partial x_n} F_j & \cdots \end{pmatrix} \tag{4.14}$$

and

$$W_A = (\cdots W_{Aj} \cdots)^T, \quad W_B = (\cdots W_{Bj} \cdots)^T \tag{4.15}$$

and

$$W_{Aj} = \frac{\int_0^\pi \frac{\partial \lambda_j}{\partial \beta_j} d\beta_j}{\int_0^\pi \lambda_j d\beta_j} \tag{4.16}$$

$$W_{Bj} = \frac{\int_0^\pi \frac{\partial \lambda_j}{\partial \beta_j} \cos\beta_j \, d\beta_j}{\int_0^\pi \lambda_j d\beta_j} \tag{4.17}$$

Also, it follows that

$$\overline{\underline{\varphi}} = \langle \Lambda \Lambda^T \mid \gamma_n = \gamma \rangle \tag{4.18}$$

$$= D_A H_{WA} D_A^T + D_A H_{WAB} D_B^T - (D_A H_{WAB} D_B^T)^T + D_B H_{WB} D_B^T \tag{4.19}$$

where

$$H_{WA} = \underset{d}{Diag}(h_{WA1}, h_{WA2}, \cdots h_{WAJ}) \tag{4.20}$$

$$H_{WB} = \underset{d}{Diag}(h_{WB1}, h_{WB2}, \cdots h_{WBJ}) \tag{4.21}$$

$$H_{WAB} = \underset{d}{Diag}(h_{WAB1}, h_{WAB2}, \cdots h_{WABJ}) \tag{4.22}$$

(where Diag. means diagonal) and

$$hw_{Aj} = \langle W_{Aj}^2 \mid r_u = r \rangle \tag{4.23}$$

$$hw_{Bj} = \langle W_{Bj}^2 \mid r_u = r \rangle \tag{4.24}$$

$$hw_{ABj} = \langle W_{Aj} W_{Bj} \mid r_u = r \rangle \tag{4.25}$$

The functions w_A, w_B, Hw_A, Hw_B, and Hw_{AB}, resulting from the averaging, are extremely complicated. The computation of these functions was done by using numerial approximation on a digital computer. The table lookup technique was used in computing Hw_A, Hw_B, and is discussed in the next chapter.

CHAPTER 5

TABLE LOOKUP TECHNIQUE

In the development of the suboptimal receiver we need to calculate the values of the functions Hw_A, Hw_B, and Hw_{AB}, which were defined in (4.20), (4.21), and (4.22). Their complex nature is such that they cannot be calculated in real time because of the excessive length of the required calculation; for example, it requires 16 minutes to calculate a set of three functions for a specific set of q_{Aj} and B_j on the PDP-11 minicomputer and 24 seconds on a CDC 6400 computer. In a complete simulation run the values of these functions for 6,500 different sets of q_{Aj} and B_j are required. The required time spent limits the practical value of this approach at present.

Two approaches were considered to solve this problem. One method is to use simple functions which can be computed quickly to approximate these complicated functions; the second one is the use of a table lookup technique.

Both approaches need the values of the functions themselves to proceed. We first chose some even-spaced values of q_A and B to generate the values of those functions and plot them. Here, it was necessary to use smooth interpolation to complete the plots; the interpolation was also used in the table lookup procedure. Six plots, Hw_A vs. q_A, Hw_B vs. B, Hw_{AB} vs. q_A, Hw_{AB} vs. B, Hw_B vs. q_A, and Hw_B vs. B, were made. From

these approximate plots, i.e. plots of equally chosen increments, the reference values of q_A and B were then determined more specifically to build more accurate plots. The plots were used to find the approximation functions, if any, and to decide the reference coordinate intervals for the table lookup technique.

It was seen, from the plots, that these functions were too complicated and irregular to be approximated by simple functions. At this point, approximation functions were investigated for their potential. While they were often found to be close to the real functions, they still did not satisfactorily reflect the characteristics of the real functions.

Several things had to be considered in employing the table lookup technique:

1. Would linear interpolation, polynomial interpolation, or other kinds of interpolation be used?
2. Would some modification of the true functions, e.g. square root values, logarithmic values, or exponential values, be better in interpolation than the true values?
3. How would the reference points be chosen?

In this case it is necessary to extend the one-dimensional interpolation to the two-dimensional interpolation, since the functions were of two variables.

It was desired to find the simplest interpolation method whose deviation was tolerable. Linear interpolation of logarithmic values of Hw_A and Hw_B and of actual values of

$$B_{AB} \triangleq \frac{H_{wAB}}{\sqrt{H_{wA}\, H_{wB}}} \tag{5.0}$$

were shown to provide deviations generally less than ten percent.

In defining reference points for the interpolation intervals the standard procedure demands large intervals in slowly varying ranges and small intervals for rapidly varying ranges. The range and reference points finally chosen were

$$-.99 \leq B \leq .99 \tag{5.1}$$

$$.1 \leq q_A \leq 10^8 \tag{5.2}$$

and 11 intervals for B with reference points 0.01, 0.02, 0.04, 0.06, 0.01, 0.02, 0.03, 0.05, 0.07, 0.09, 0.95, and 0.99. Also chosen were 24 intervals for q_A with reference points 0.1, 0.1778, 0.3162, 0.5623, 1, 1.778, 3.162, 5.623, 10, 17.78, 31.62, 56.23, 100, 177.8, 316.2, 562.3, 1000, 1778, 3162, 5623, 10^4, 10^5, 10^6, 10^7, and 10^8. A table of 300 values was then constructed as the first step in the table lookup procedure.

The next step concerned the search problem. Whenever a set of q_A and B was obtained, it was necessary to determine in what interval it belonged. Two search methods were tried. The binary search was the first. Assuming there was no correlation among different q_A and B values, the binary search was conducted by successfully dividing the range into two equal parts. Another method, which was termed "the

presearch method," assumes a positive correlation between successive values of q_A and B. The current search started with the previous interval and was then followed by a linear search. Since q_A and B were generated randomly, experiments were necessary to determine which method proved most efficient in our simulation runs. The results showed that the "presearch method" was the fastest· thus, this method was used in the table lookup subroutine.

The final step was to follow the linear interpolation formula

$$f(x_1+\Delta x, y_1+\Delta y) = f(x_1,y_1) + \frac{f(x_2,y_1)-f(x_1,y_1)}{x_2-x_1}\Delta x + \frac{f(x_1,y_2)-f(x_1,y_1)}{y_2-y_1}\Delta y + \left[f(x_1,y_1)+f(x_2,y_2)-f(x_1,y_2)-f(x_2,y_1)\right]\frac{\Delta x\,\Delta y}{(x_2-x_1)(y_2-y_1)} \tag{5.3}$$

to obtain the desired values.

CHAPTER 6

SIMULATION STUDIES FOR THE SUBOPTIMAL RECEIVER

Components of the simulation are:

1. The environment and baseband receiver signal.
2. The LOE/Kalman filter recursive receiver structure and, specifically, both multipath-adaptive and non-adaptive variants.
3. A representation of the Phase III MLS receiver denoted the threshold receiver.

Simulation studies conducted, which focused on the suboptimal receiver, included the following:

A. Crossing multipath interference and comparison for all receivers.

B. RMS error versus $\theta_{sep} \triangleq \theta - \theta_R$ and comparison for all receivers.

C. Acquisition scenario for the suboptimal receiver.

Simulation models are discussed first and then results presented.

Simulation Models

Environment and Baseband Receiver Signal

Basically, the environmental dynamics are simulated with a state model of the form (2.8), without the random excitation, using the state

vector, x, (2.1); however, the observations are generated in absolute-amplitude form. So, the full model is

$$X(K+1) = FX(K), \qquad X(0) = X_0 \tag{6.1}$$

$$V(K) = h_V(x(K), \sigma, n(K)) \tag{6.2}$$

where

X_0 = the initial state at the start of the simulation (6.3)

$$F \triangleq \begin{pmatrix} 1 & 0 & 0 & 0 & 0 & 0 & 0 & 0 \\ 0 & 1 & T_K & 0 & 0 & 0 & 0 & 0 \\ 0 & 0 & 1 & 0 & 0 & 0 & 0 & 0 \\ 0 & 0 & 0 & 1 & 0 & 0 & 0 & 0 \\ 0 & 0 & 0 & 0 & 1 & T_K & 0 & 0 \\ 0 & 0 & 0 & 0 & 0 & 1 & 0 & 0 \\ 0 & 0 & 0 & 0 & 0 & 0 & 1 & T_K \\ 0 & 0 & 0 & 0 & 0 & 0 & 0 & 1 \end{pmatrix} \tag{6.4}$$

σ = rms value of receiver noise at a point in the I-F channel having the same signal amplitude as the demodulator output. (6.5)

The parameter σ is assumed known, being a receiver characteristic.

$h_V(\,)$ = a matrix-valued function of its arguments, which compiles the J vector v(k) as one with a representative element $V_j(K)$, $j = 1, 2, \ldots J$. (6.6)

where

$$V_j(K) = \sigma\sqrt{2\mu_j} \tag{6.7}$$

and u_j is as given in (2.9).

Signal data samples are generated only during sampling windows of J/2 samples each, located in the TO and FRO scans, respectively, and centered where the centroid of the receiver signal pulses are expected. For all runs to date

$$J = 130 \tag{6.8}$$

corresponding to window width of eight degrees in each semiscan.

The Optimal Receiver Simulation

The optimal receiver simulation consists basically of the following:

1. Extrapolation of $\hat{x}$ to the present, via (3.10). (6.9)
2. Scan data processor calculation of Λ, via (3.33), and Ξ, via (3.34). (6.10)
3. Kalman filter calculation as follows:
   a. $P(K|K-1)$, via (3.11) (6.11)
   b. Gain matrix, M(k), via)3.23). (6.12)
   c. $\hat{X}(K|K)$, via (3.22). (6.13)
   d. $P(K|K)$, via (3.26). (6.14)

The Suboptimal Receiver Simulation

The suboptimal receiver used the same procedure as the optimal

receiver, but the calculations of Λ and Φ were different. Calculation of Λ follows (4.13), and that of Φ follows (4.19).

The Antenna Selectivity Function

The following antenna selectivity function, $p(\theta)$, and its derivative $\dot{p}(\theta)$ were used in both the optimal and the suboptimal simulation runs;

$$p(\theta) = \begin{cases} \pi/4 & \theta = B/2.4 \\ \dfrac{\cos(1.2)\pi\theta/B}{1-(2.4\theta/B)^2} & \text{elsewhere} \end{cases} \tag{6.15}$$

and

ORIGINAL PAGE IS
OF POOR QUALITY

$$\dot{p}(\theta) \begin{cases} -\dfrac{0.3\pi}{B}\,\mathrm{sign}(\theta), & \theta = B/2.4 \\ \dfrac{0.3\pi^2}{B}\left\{ \cos\dfrac{\pi}{2}(z+1) - \dfrac{\sin(\frac{\pi}{2}(z+1))}{(\pi/2)(z-1)} + \dfrac{\cos\frac{\pi}{2}(z-1) - \dfrac{\sin(\frac{\pi}{2}(z-1))}{(\pi/2)(z-1)}}{\pi/2\,(z-1)} \right\} & \text{elsewhere} \quad z = \dfrac{2.4\theta}{B} \end{cases} \tag{6.16}$$

in which B, the 3 dB beam width in degrees, was given the value of one degree.

Threshold Receiver

Performance of the threshold receiver was included in the data for comparison. Reference about the threshold receiver can be found in the

paper by R. J. Kelly [6].

Simulation Runs and Results

The following four parameters are important to the performance of an MLS receiver.

$S/N \triangleq$ Direct-path signal-to-noise ratio (dB) (6.17)

$\rho \triangleq$ Multipath to direct-path signal amplitude ratio (6.18)

$f_{sc} \triangleq$ Scalloping frequency (H_Z) (6.19)

$\theta_{sep} \triangleq \theta - \theta_{ref}$, the separation angle between multipath and direct-path direction (6.20)

The MLS receivers are expected to operate with S/N ratio of 8 dB or higher. Values in the range 8 to 20 dB were used in the simulation study.

Another parameter, β, the initial r-f phase difference between direct-path and multipath signals, also affected the results.

Crossing Multipath Studies

This scenario began with

$$\theta_{sep} = -2.75^\circ \quad (6.21)$$

$$\frac{d\theta_{sep}}{dt} = 0.7^\circ/sec \quad (6.22)$$

and ran for 100 scans (approximately 7.4 seconds). Runs corresponding to

different values of parameters S/N, ρ , and fsc were made. In this scenario we assumed all runs were intitialized in the track mode, i.e. all estimated variables produced by each receiver were intitialized to true value. Figures 6.1 through 6.9 show the angle estimation errors of the suboptimal, optimal, and threshold receivers and the composite SNR as functions of time and separation angle. It should be remembered that the separation angle $\theta_{sep} = -275 + \int \frac{d\theta_{sep}}{dt} dt$

The key parameters S/N, ρ (RHO), β (BETA), fsc(FSC), and the rms errors are on the bottom of each plot. Figure 6.1 presents time histories of error for S/N = 20 dB, $\rho = 0$, i.e. no multipath interference. Figure 6.2 shows the same case, with the multipath signal half as large as the direct-path signal. Note that the performance is better for the suboptimal and optimal receivers in the case of multipath interference. Figures 6.3, 6.4, and 6.5 present the time histories for $\beta = 180°$, fsc = 500 under different SNR and ρ . Figures 6.6 through 6.9 present the cases with fsc = 51.3 Hz, $\beta = -168°$, which produce maximum enhancement by the multipath on the TO scan and maximum cancellation on the FRO scan [7]. It is clear that the optimal receiver generally performed the best and the suboptimal outperformed the threshold receiver.

Tables 1 and 2 summarize some interesting features from Figs. 6.2 through 6.9.

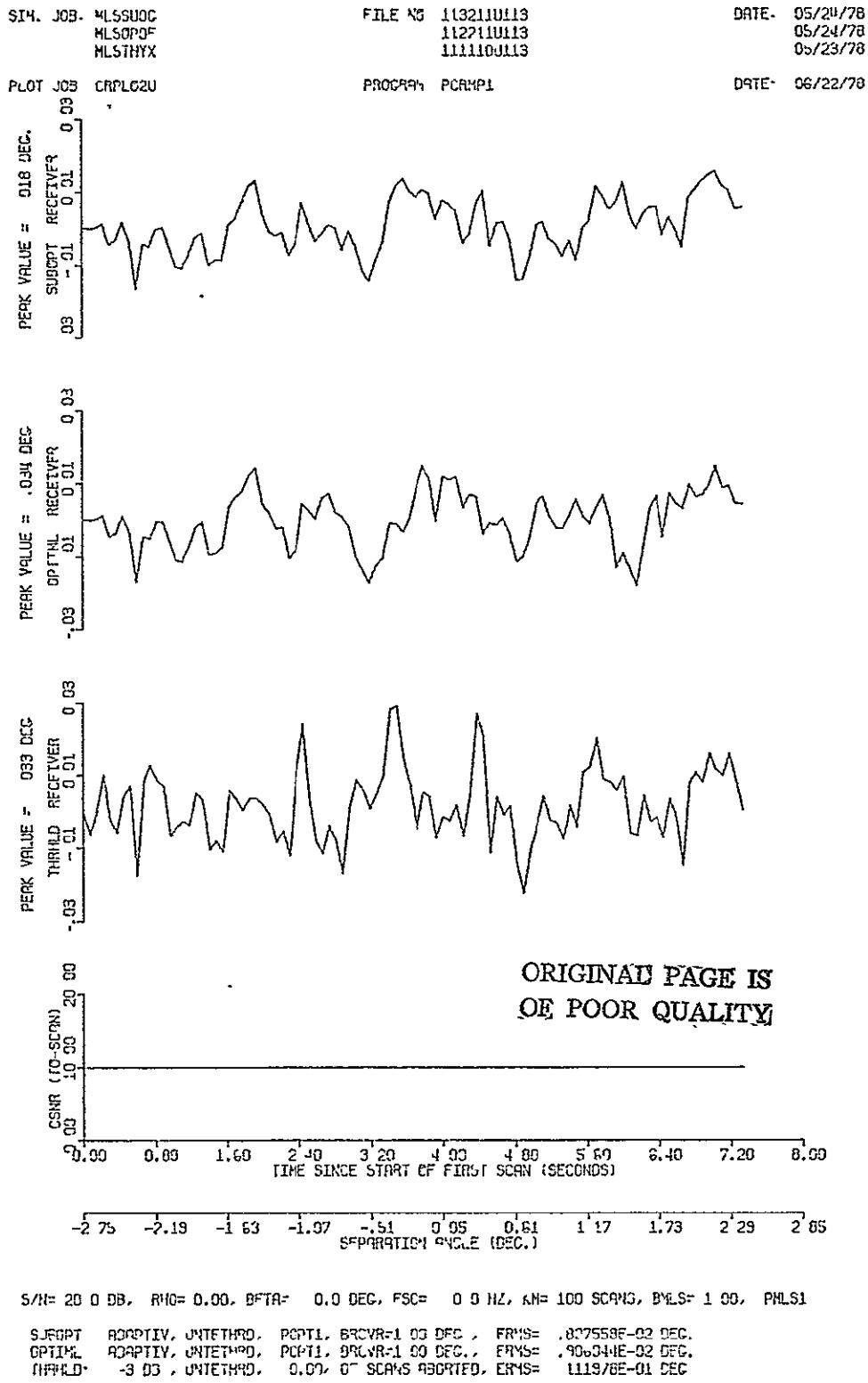

Fig. 6.1

Crossing Multipath Scenario. Reference Case: High S/N; No Interference.

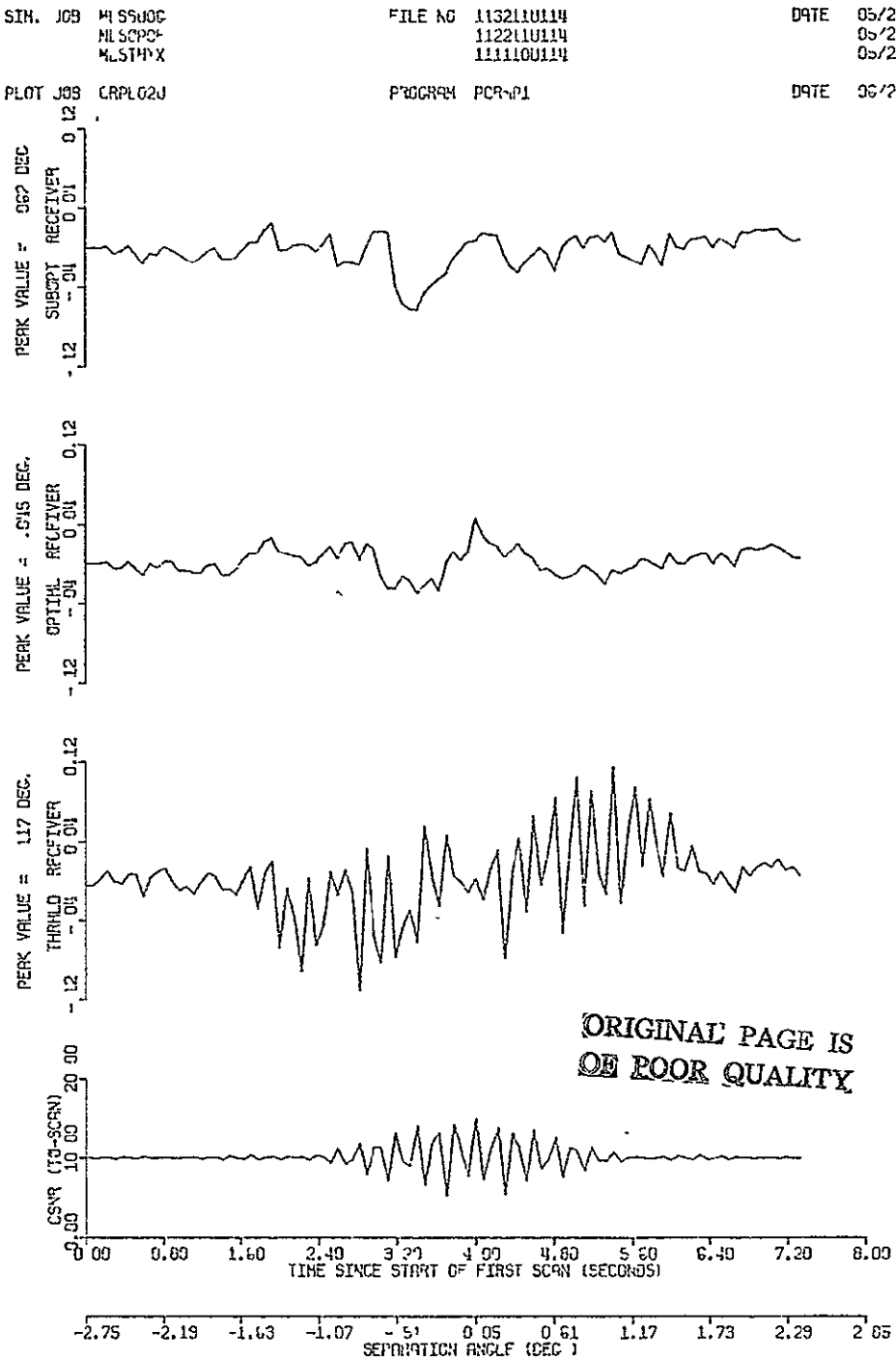

Fig. 6.2

Crossing Multipath Scenario; High S/N,
Moderate Interference, Low Scalloping Rate

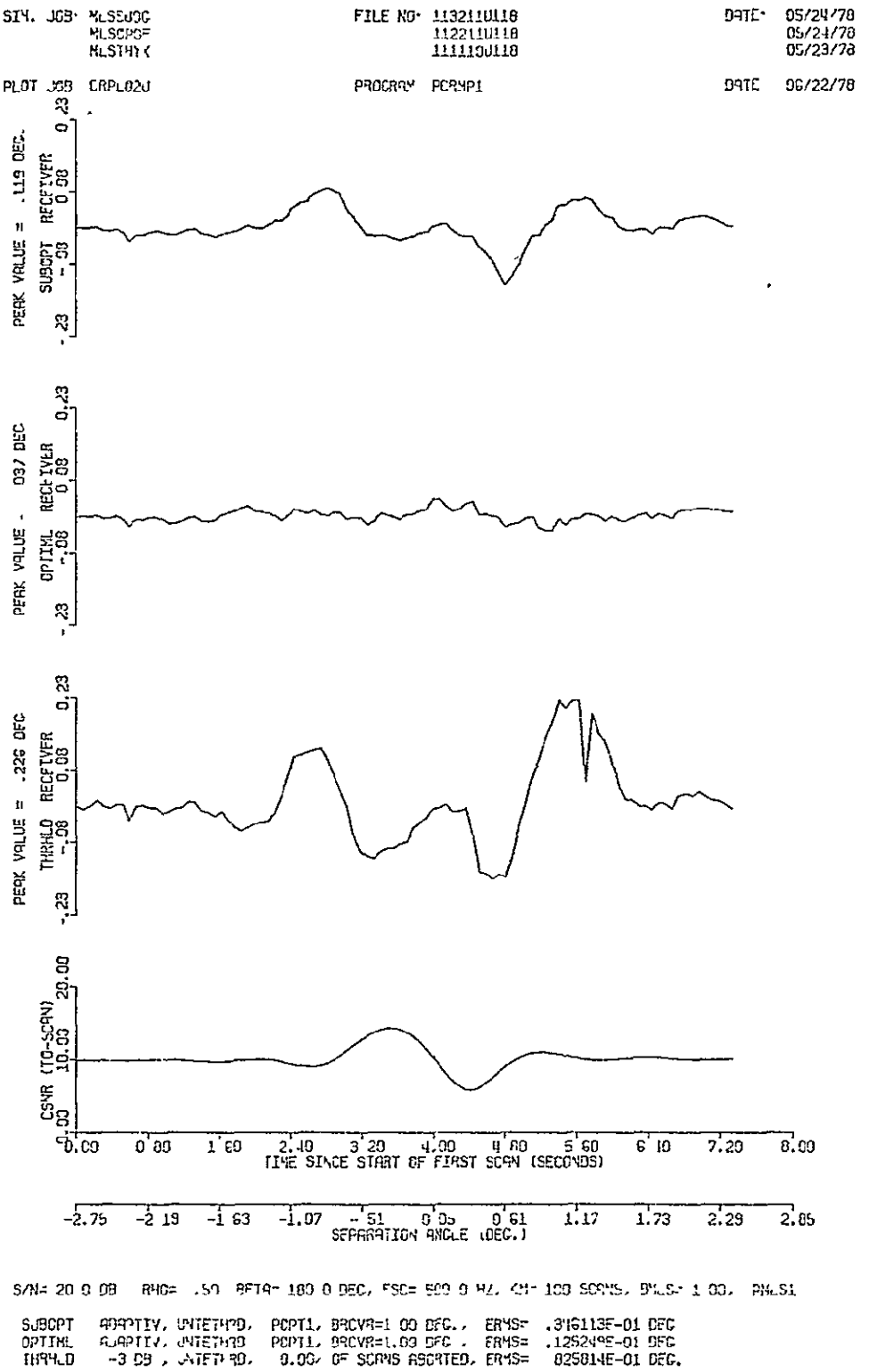

Fig. 6.3

Crossing Multipath Scenario; High S/N, Moderate Interference, High Scalloping Rate

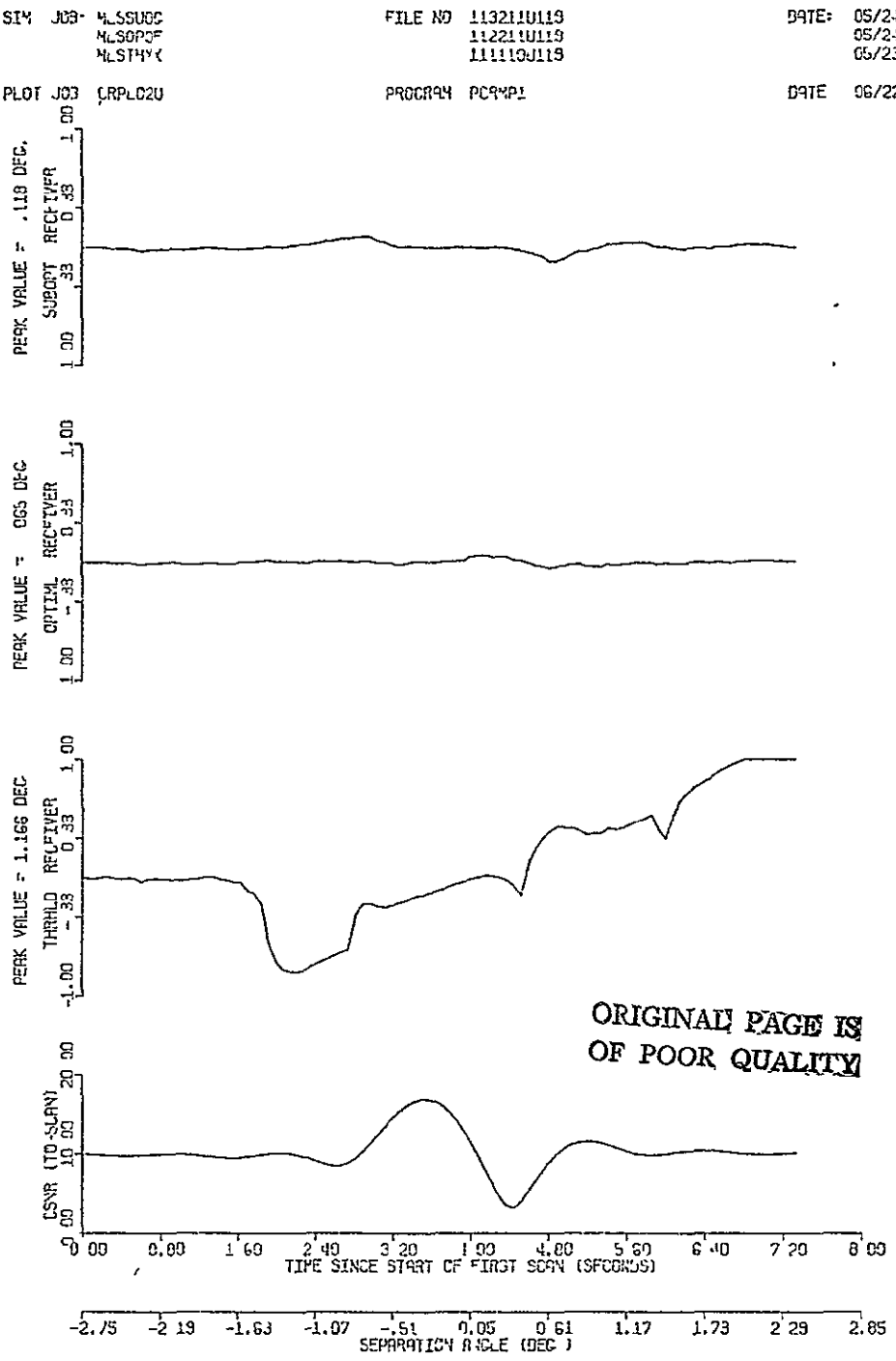

Fig. 6.4

Crossing Multipath Scenario; High S/N,
Heavy Interference, High Scalloping Rate

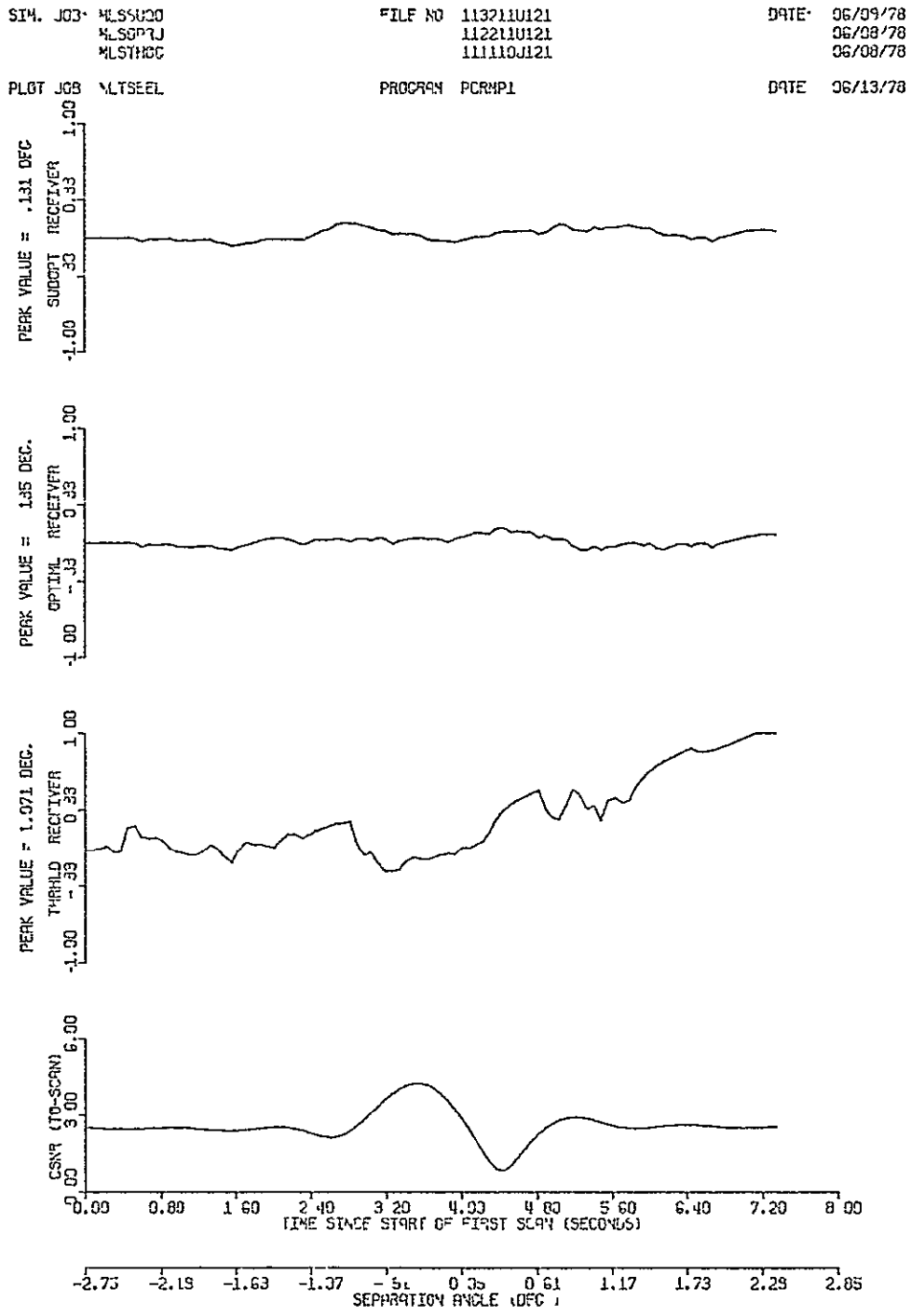

Fig. 6.5

Crossing Multipath Scenario; Low S/N,
Heavy Interference, High Scalloping Rate

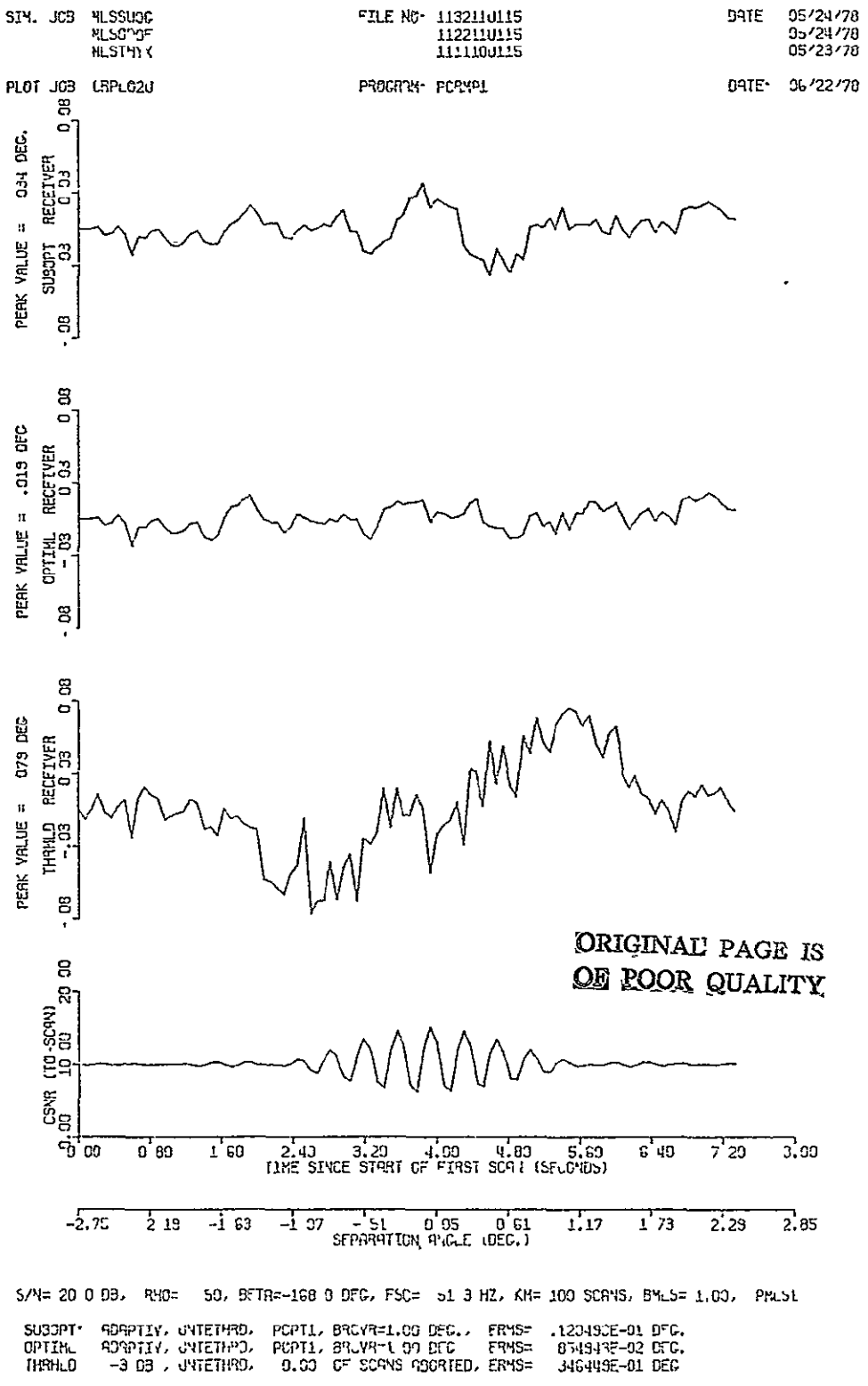

Fig. 6.6

Crossing Multipath Scenario; High S/N,
Moderate Interference, Moderate Scalloping Rate

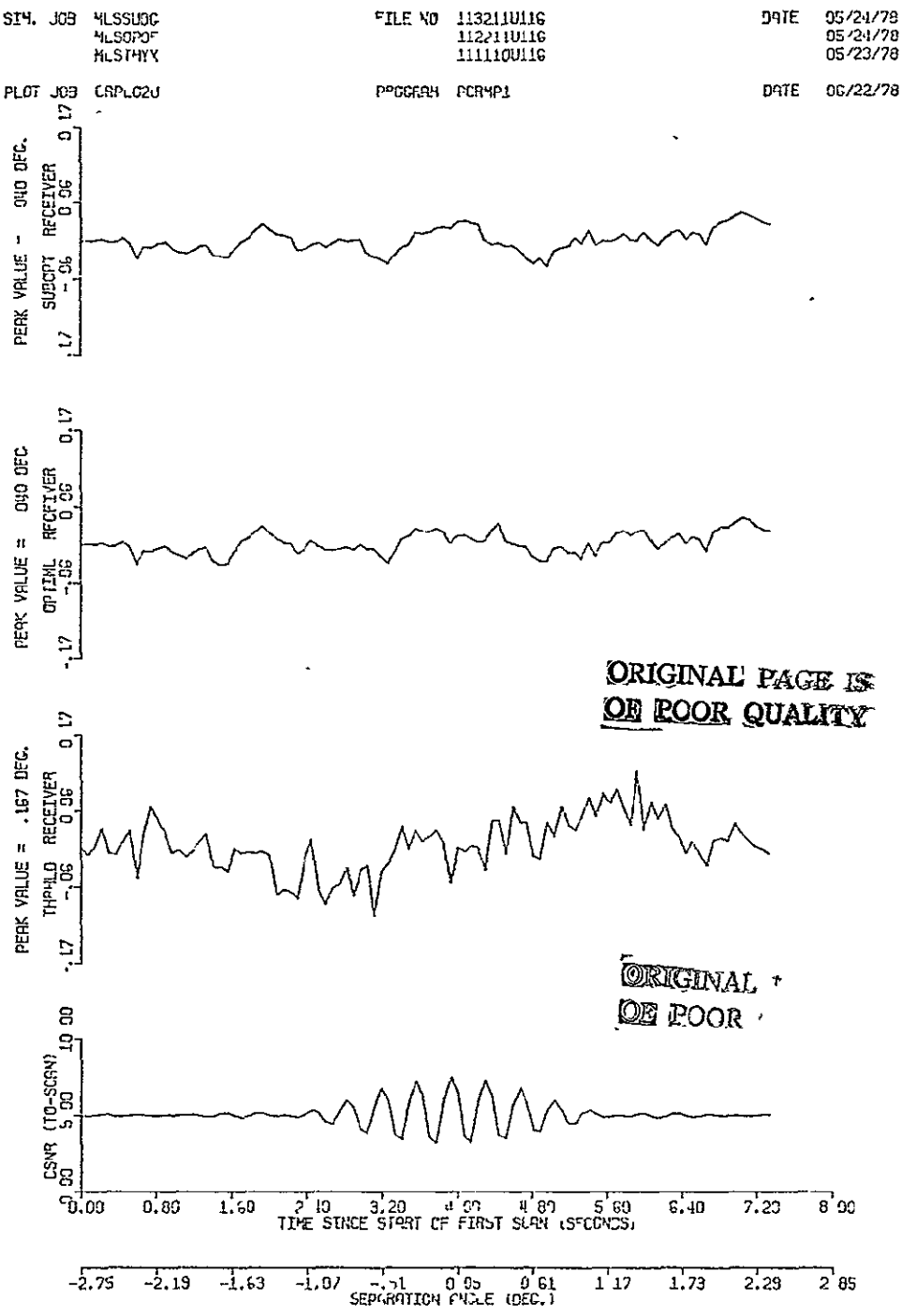

Fig. 6.7

Crossing Multipath Scenario; Moderate S/N
Moderate Interference, Moderate Scalloping Rate

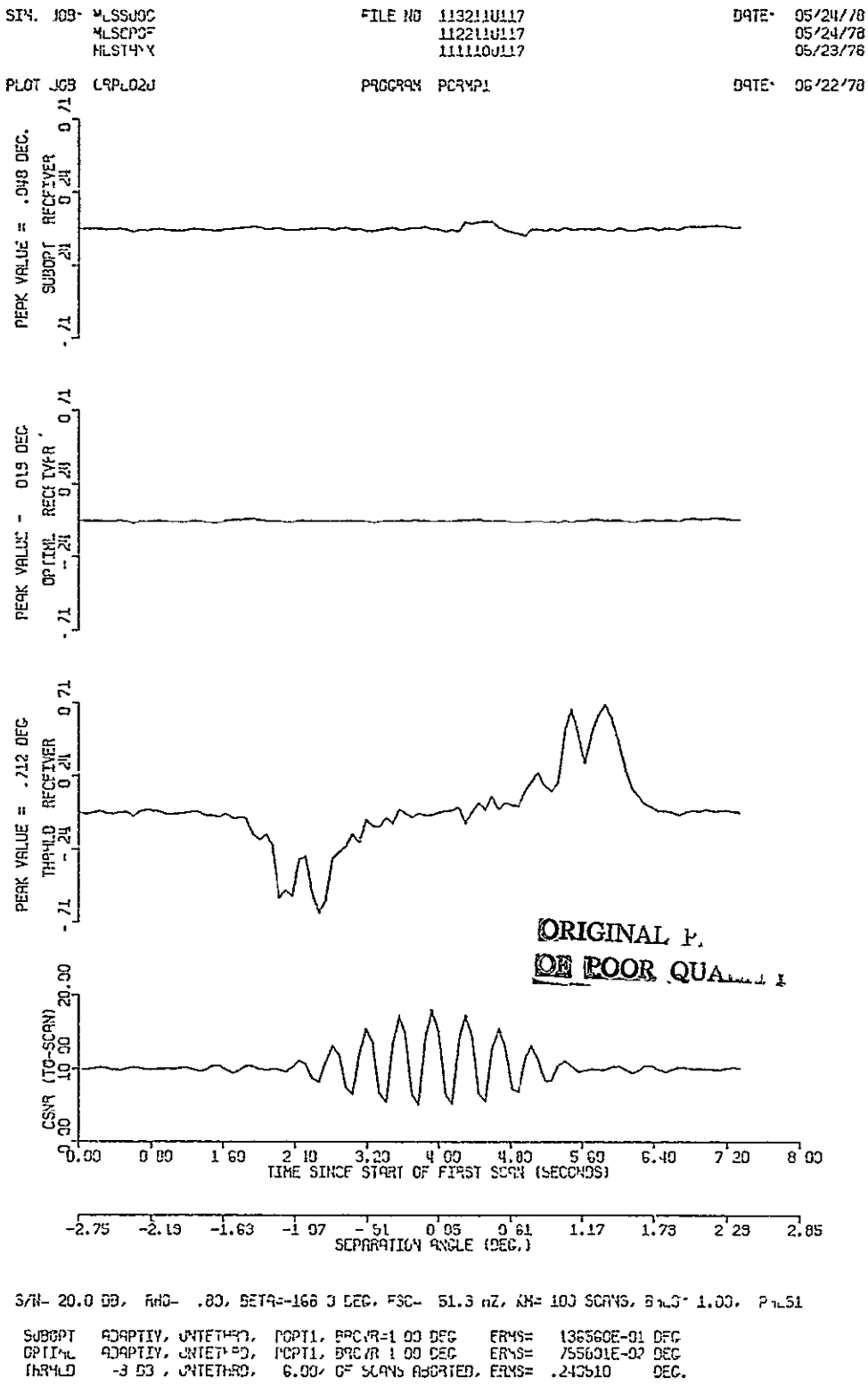

Fig. 6.8

Crossing Multipath Scenario, High S/N,
Heavy Interference, Moderate Scalloping Rate

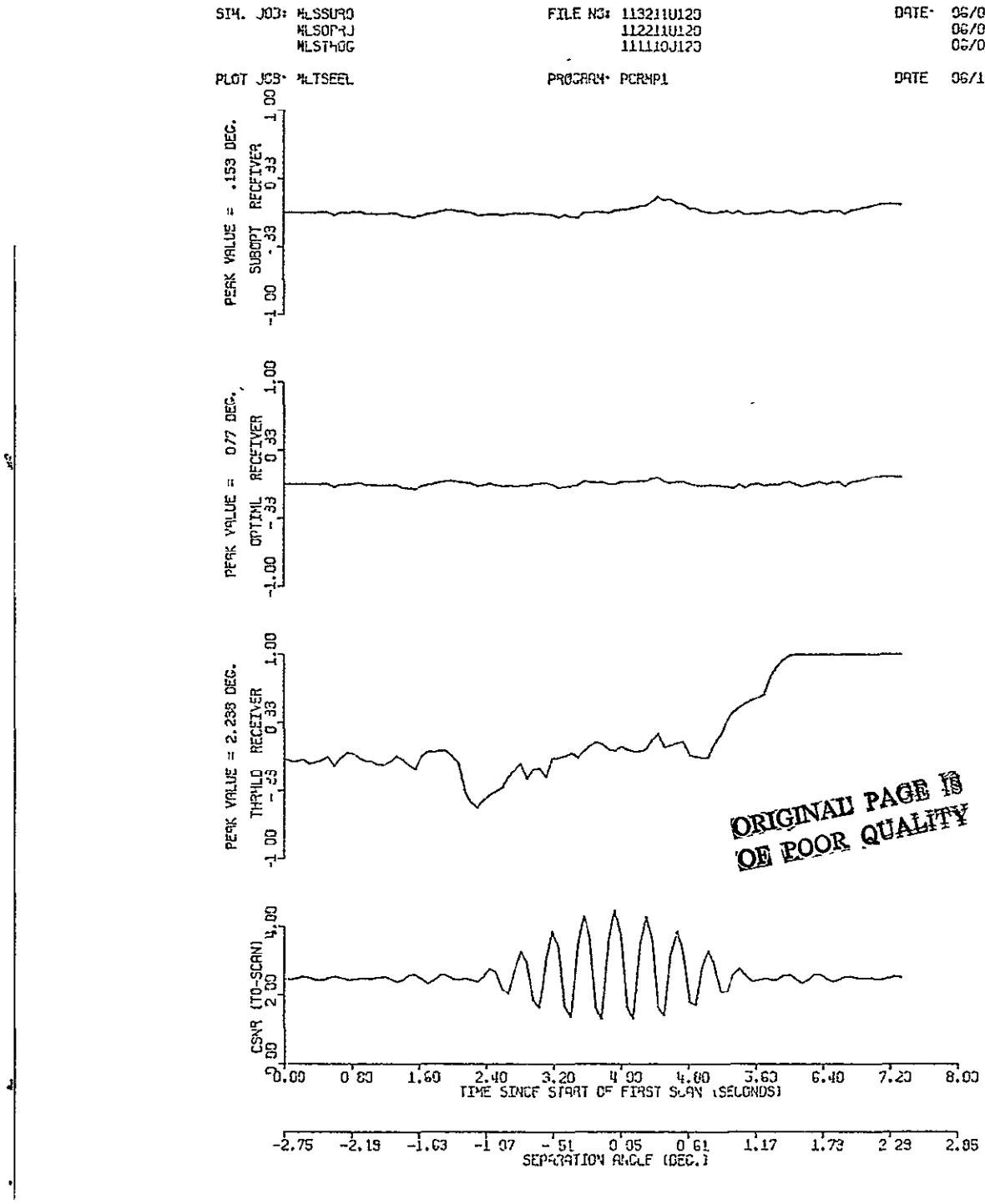

Fig. 6.9

Crossing Multipath Scenario; Low S/N,
Heavy Interference, Moderate Scalloping Rate

TABLE 1

SNR	β	fsc	ρ	RMS Error		
				Thr.	Opt.	Sub.
20 dB	-168	51.3	.8	.243	.026	.039
			.5	.035	.0085	.012
	-180	500	.8	.51	.019	.035
			.5	.083	.013	.035

TABLE 2

β	fsc	ρ	SNR	RMS Error		
				Thr.	Opt.	Sub.
-168	51.3	.5	20	.035	.0085	.034
			14	.043	.016	.040
		.8	20	.24	.0076	.014
			8	.77	.0265	.039
-180	500	.8	20	.51	.019	.035
			8	.439	.045	.054

From Table 1, we saw that the performance of the threshold receiver is more sensitive to the multipath to direct-path ratio than the suboptimal and optimal receivers. From Table 2, we noticed that higher SNR generally gave better performance and that the SNR affected each receiver to about the same extent.

RMS Error Studies

These data are sample RMS values calculated for the θ error processes of the three receivers by taking averages over 100 scans of simulation results run in environments that are stationary, except the phase angle β. The scalloping rate used swept β over a 2π interval during the 100 scans, thus rendering the averages taken as sample means with respect to both noise and β. The first ten scans in each run were excluded from the averaging to minimize transient effects in the computation. The results are presented as functions of θ_{sep}, parameterized by S/N and ρ, as indicated on the various figures.

The comparative performances elicited by these tests were not entirely satisfying in view of the striking contrasts produced by the crossing multipath studies. This outcome may be due, in part, to the way aborts are processed in the threshold receiver simulation (immediate reset of the state estimate to the true state on abort), but the data clearly indicates some performance deficiencies in this environment of the optimal and suboptimal receivers, as currently structured. Subsequent re-examination of the results of these runs and others indicate the optimal and suboptimal receivers, at small separation angles,

occasionally, at some point in the 100-scan averaging interval, would shift to a false-lock null or lose track completely. This is believed to be correlated with the sweeping of β over a 2π interval during the 100-scan averaging process. The performance results, given in Figs. 6.10 through 6.15, appear to be representative of the optimal and suboptimal receivers, as presently structured. Elimination of the problems noted may require some restructuring of the receiver, possibly reverting to the "nonadaptive' design when an interference pulse is not both present and distinct from the direct-path pulse. This problem is under consideration presently.

Acquisition Scenario

There are five parameters, α, ϑ, α_R, θ_R, and β, in the parameter vector γ which is to be estimated in the optimal receiver. If the multipath signal occurs while the receiver is tracking the direct-path signal, acquisition of the multipath signal may not occur. The acquisition of the parameter β, still unmanageable. prompted us to eliminate by averaging β out of γ; however, in the suboptimal receiver $\gamma = (\alpha, \vartheta, \alpha_R, \theta_R)$ can be acquired. We studied the acquisition scenario for the suboptimal receiver and presented the results in Figs. 6.16 through 6.19.

All figures present the estimation error time histories, respectively, in α, ϑ α_R, and θ_R, with the bottom trace on each, showing the time history of the ratio α_R/α. Fig. 6.16 in which the receiver was initially tracking both the direct path and multipath signals with $\theta_{sep} = 1.8\tilde{\gamma}^c$ was used for comparison. Fig. 6.17 in which the multipath signal did not occur until the 26th scan presented similar estimation

SIM JOB MLSSUF0 FILE NO 2132110101 DATE: 06/20/78
MLSOPP0 2122110101 06/19/78
MLSTHRL 2111103101 06/19/78
PLOT JOB MSPLOU8 PROGRAM PMSMP1 DATE 06/27/78

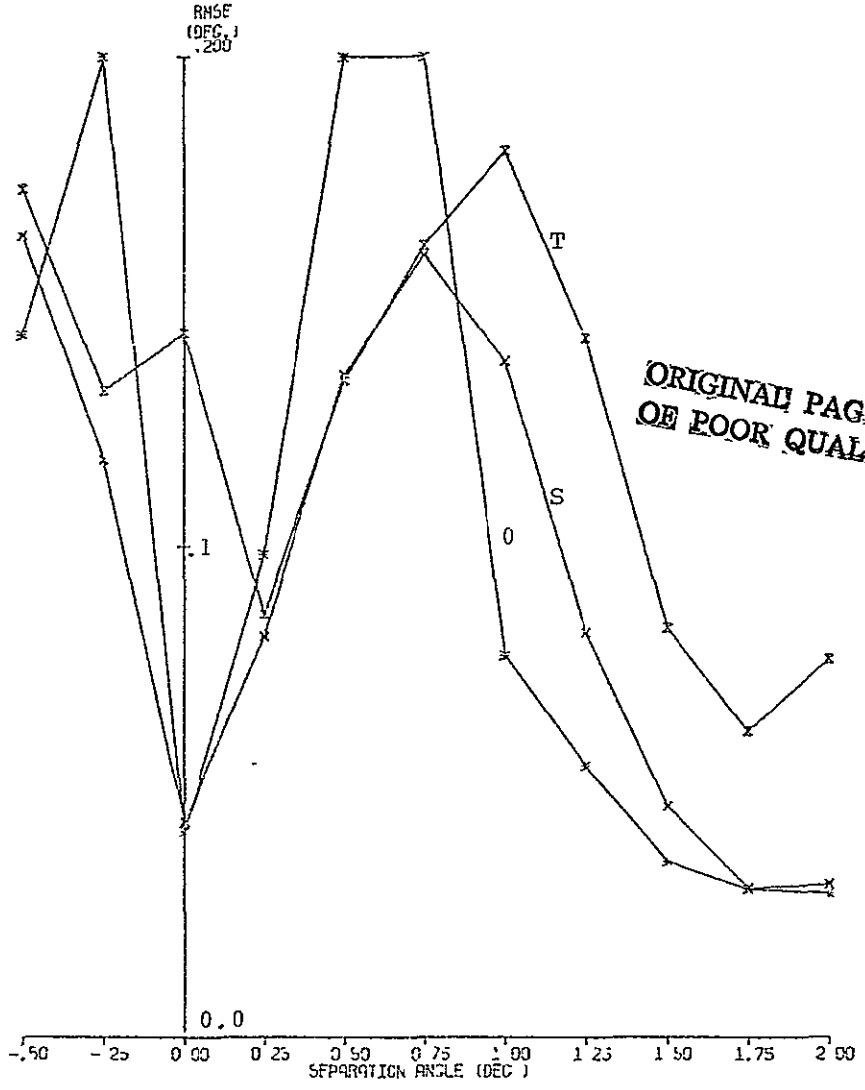

X SUBOPT ADAPTIV, UNTETHRD, DELT= .074074 SEC, POPT1, BRCVR=1.00
PMLS1, BMLS=1.00, S/N= 8.0 DB, RHO= .5, FSC= 135 HZ, NTIMES= 1, LGMAX=13, KM=110

X OPTIML ADAPTIV, UNTETHRD, DELT= .074074 SEC, POPT1, BRCVR=1.00
PMLS1, BMLS=1.00, S/N= 8.0 DB, RHO= .5, FSC= 135 HZ, NTIMES= 1, LGMAX=13, KM=110

X INITLD -3.03 , UNTETHRD, DELT= .074074 SEC, MAX. ABORTS= 25 36 > 91 TMESEP= .75 DEG
PMLS1, BMLS=1.00, S/N= 8.0 DB, RHO= .5, FSC= .135 HZ, NTIMES= 1, LGMAX=13, KM=110

Fig. 6.10

RMS Error Studies; Low S/N, Moderate Interference

SIM JOB MLSSUIK FILE NO 213211U102 DATE: 06/23/78
MLSOPJ2 212211U102 06/21/78
MLSTH90 211110U102 06/21/78
PLOT JOB MSPLOU3 PROGRAM. PMSMP1 DATE: 06/27/78

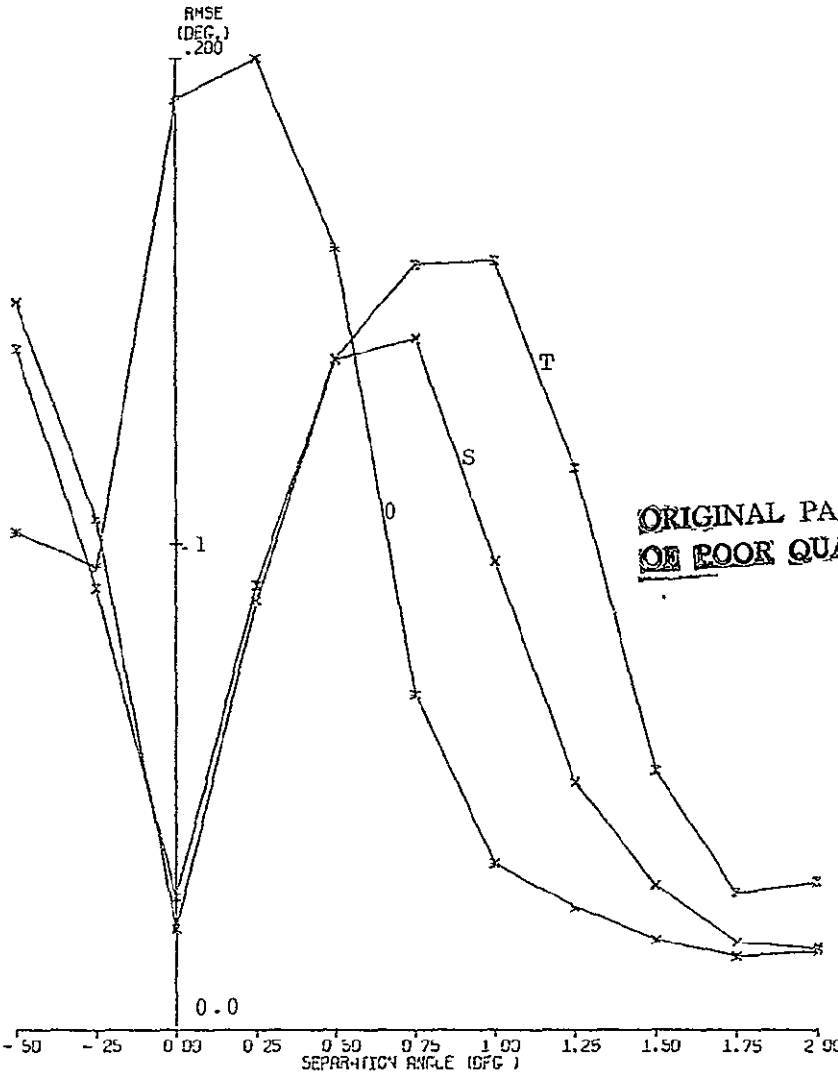

X SUBOPT- ADAPTIV, UNTETHRD, DELT= .074074 SEL POPT1, BRCVR=1.00
P-LS1, B-LS=1.00, S/N= 14.0 DB, RHO= .5, FSC= 135 HZ, MTIMES= 1, LGMAX=13, KM=110

> OPTIMU ADAPTIV, UNTETHRD, DELT= .074074 SEL, POPT1, BRCVR=1.00
PMLS1, B-LS=1.00, S/N= 14.0 DB, RHO= .5, FSC= 135 HZ, MTIMES= 1, LGMAX=13, KM=110

X THRHLD -3 DB , UNTETHRD, DELT= .074074 SEL, NOT POPTS= 6.30 , AT THETA= 1.25 DEG
PMLS1, B-LS=1.00, S/N= 14.0 DB, RHO= .5, FSC= 135 HZ, MTIMES= 1, LGMAX=13, KM=110

Fig. 6.11

RMS Error Studies; Moderate S/N, Moderate Interference

SIM JCD MLSSUIK
MLSOPJ2
MLSTM98
PLOT JOB: MSPL00B

FILE NO: 2132110103
2122110103
2111100103
PROGRAM PMSMP1

DATE 06/23/78
06/21/78
06/21/78
DATE: 06/27/78

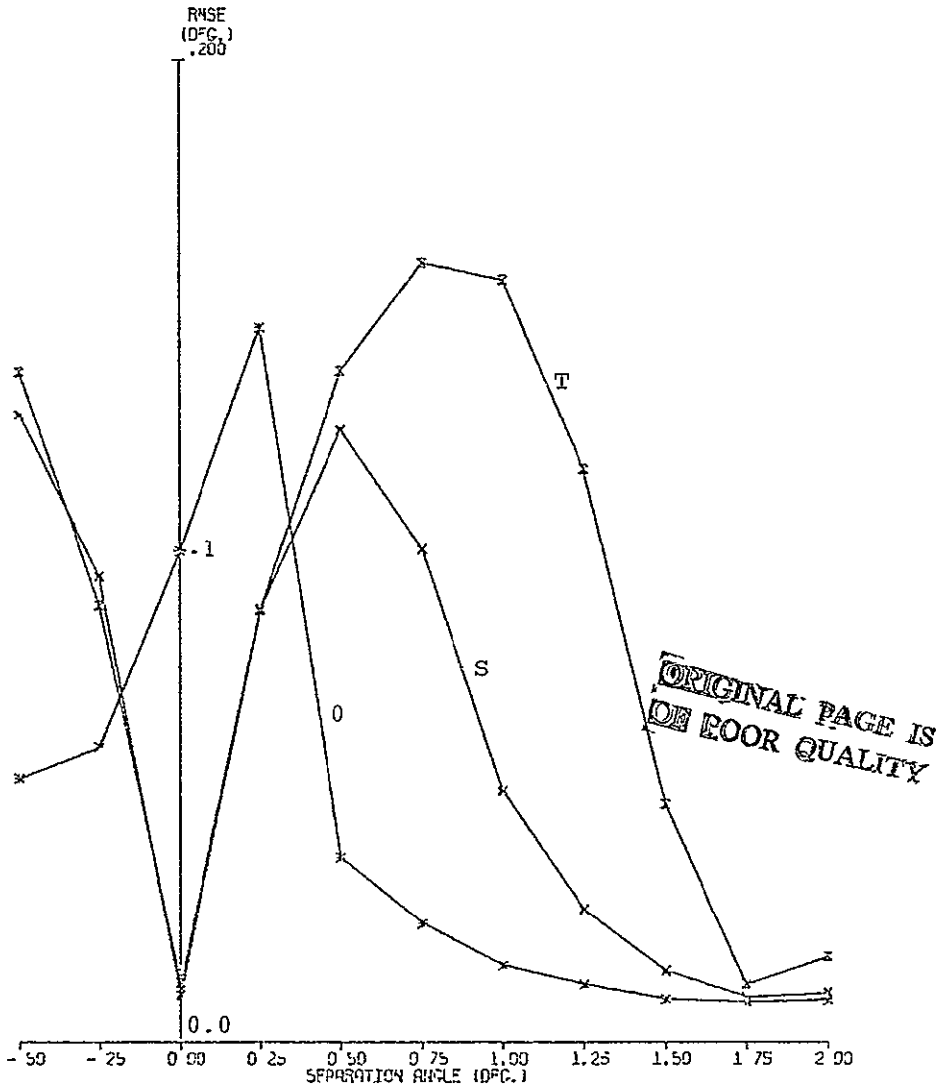

X SUBOPT ADAPTIV, UNTETHRD, DELT= .074074 SEC, PBPT1, BRCVR=1.00
PWLS1, BWLS=1.00, S/N= 20.0 DB, RHO= .5, FSC= 135 HZ, NTIMES= 1, LGMAX=13, KM=110

* OPTIML ADAPTIV, UNTETHRD, DELT= .074074 SEC, PBPT1, BRCVR=1.00
PWLS1, BWLS=1.00, S/N= 20.0 DB, RHO= .5, FSC= 135 HZ, NTIMES= 1, LGMAX=13, KM=110

X THRHLD -3.98 , UNTETHRD, DELT= .074074 SEC, MAX. ABORTS= 91 , AT THESEP= 0.00 DEC.
PWLS1, BWLS=1.00, S/N= 20.0 DB, RHO= .5, FSC= .135 HZ, NTIMES= 1, LGMAX=13, KM=110

Fig. 6.12

RMS Error Studies; High S/N, Moderate Interference

SIM. JOB: MLS5UIK FILE NO 213211U104 DATE: 06/23/78
MLSOPJ2 212711U104 06/21/78
MLSTH98 211110J104 06/21/78
PLOT JOB MSPLCOB PROGRAM: PMSMP1 DATE. 06/27/78

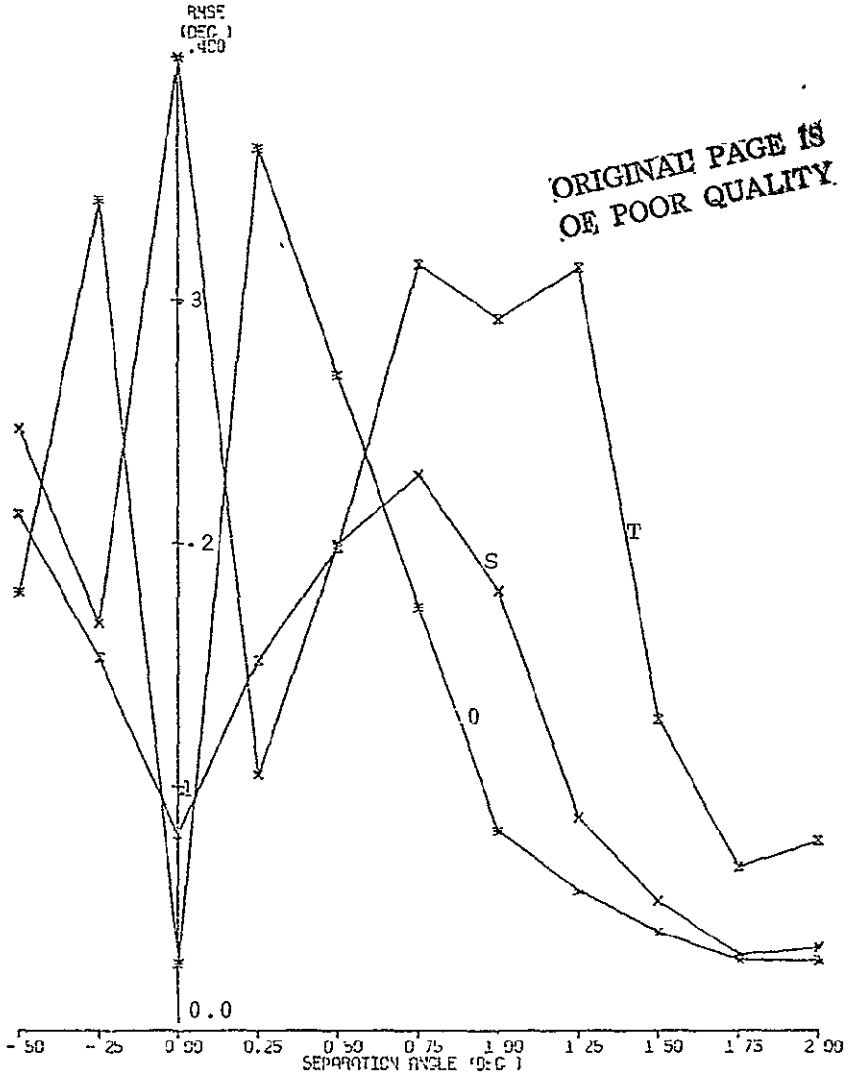

X SUBOPT ADAPTIV, UNTETHRD, DELT= 0.4074 SEC, PCPTL, BRCVR=1.00
PHLS1, BWLS=1.00, S/N= 8.0 DB, RHO= 0, FSC= .135 HZ, MTIMES= 1, LGMAX=13, KM=110

* OPTIML ADAPTIV, UNTETHRD, DELT= 0.4074 SEC, PCPTL, BRCVR=1.00
PHLS1, BWLS=1.00, S/N= 8.0 DB, RHO= 0, FSC= .135 HZ, MTIMES= 1, LGMAX=13, KM=110

X THRHLD= -3 DB , UNTETHRD, DELT= 0.4074 SEC, MAX. ABORTS= 32.73 , AT THESEP= 1.25 DEG.
PHLS1, BWLS=1.00, S/N= 8.0 DB, RHO= 0, FSC= .135 HZ, MTIMES= 1, LGMAX=13, KM=110

Fig. 6.13

RMS Error Studies; Low S/N, Heavy Interference

SIM. JOB MLSSJIK FILE NO 2132110105 DATE 06/23/78
MLSOPJ2 2122110105 06/21/78
MLSPM98 2111100105 06/21/78
PLOT JOB MSPLOJB PROGRM PMSMP1 DATE 06/27/78

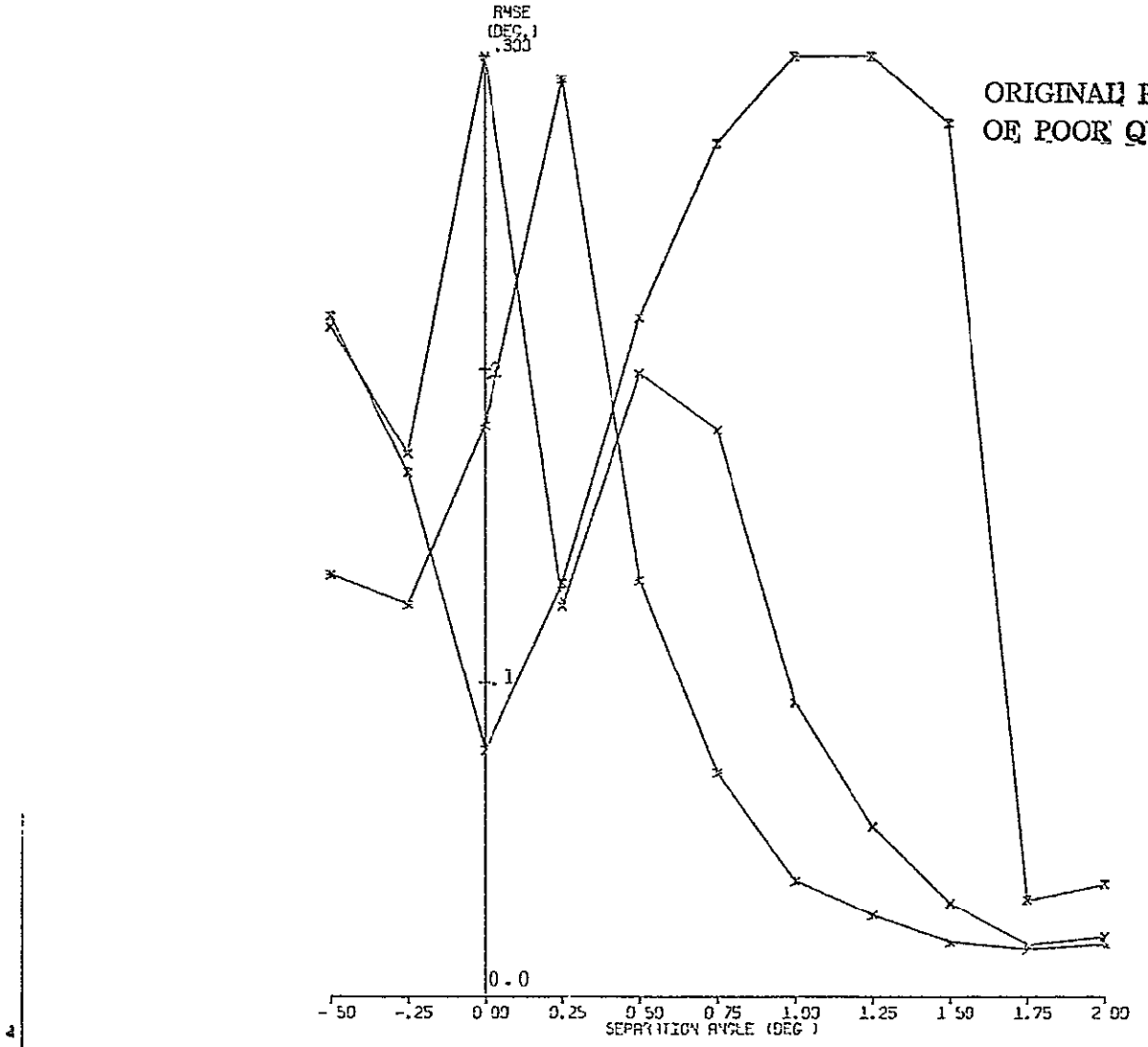

X SUBOPT ADAPTIV, UNTETHRD, DELT= .074074 SEC, POPT1, BRCVR=1.00
PMLS1, BMLS=1.00, S/N= 14.0 DB, RHO= 0, FSC= 135 HZ, MTIMES= 1, LGMAX=13, KM=110

* OPTIML ADAPTIV, UNTETHRD, DELT= .074074 SEC, POPT1, BRCVR=1.00
PMLS1, BMLS=1.00, S/N= 14.0 DB, RHO= 0, FSC= .135 HZ, MTIMES= 1, LGMAX=13, KM=110

X THRHLD -3 DB , UNTETHRD, DELT= .074071 SEC, MAX. ABORTS= 13.64 , AT THESTP= 1.25 DEG
PMLS1, BMLS=1.00, S/N= 14.0 DB, RHO= 0, FSC= .135 HZ, MTIMES= 1, LGMAX=13, KM=110

Fig. 6.14

RMS Error Studies; Moderate S/N, Heavy Interference

SIM JOB MLSSUIK FILE NO 2132110106 DATE 06/23/78
MLSPOJP 2122110106 06/21/78
MLSTM3J 2111100106 06/21/78
PLOT JOB MSPLOUB PROGRAM PMSMP1 DATE 06/27/78

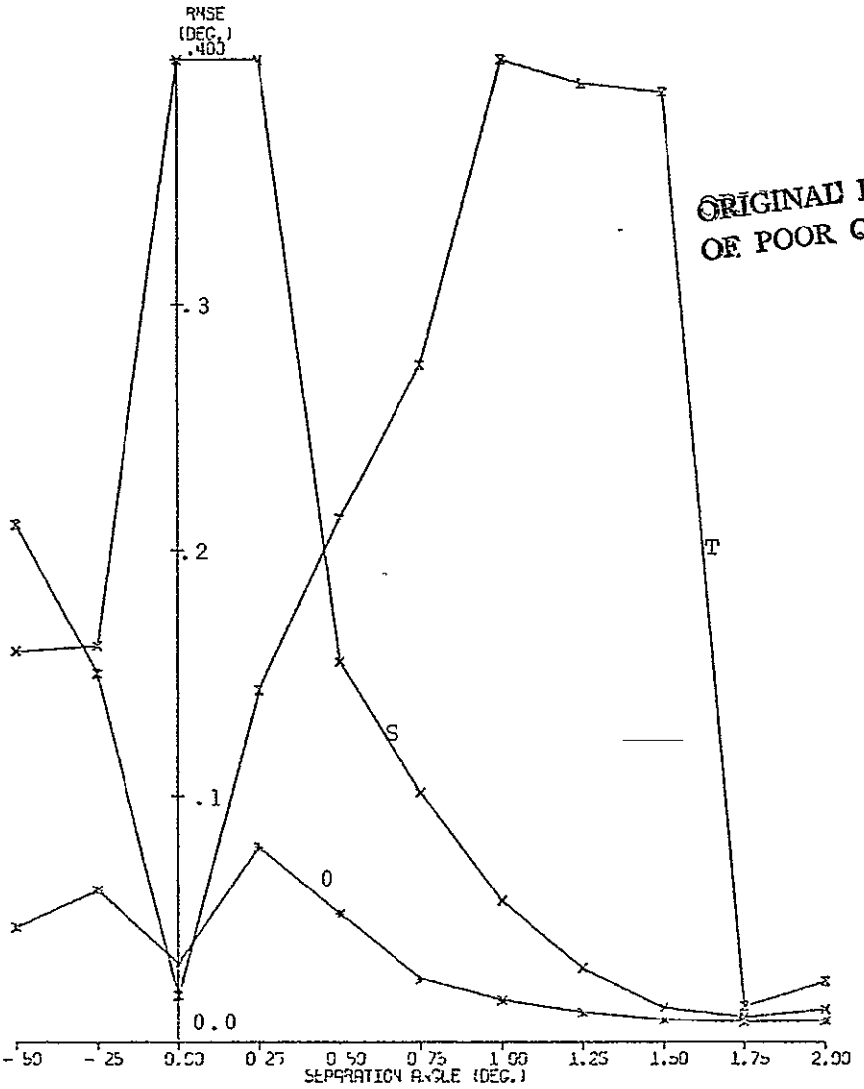

X SUBOPT ADAPTIV, UNTETHRD DELT= 074074 SEC, POPTI, BRLVR=1 00
PMLS1, BMLS=1 00, S/N= 20 0 DB, RHO= .8, FSC= .135 HZ, MTIMES= 1, LGMAX=13, KM=110

✳ OPTIML ADAPTIV, UNTETHRD, DELT= 074074 SEC, POPTI, BRLVR=1 00
PMLS1, BMLS=1 00, S/N= 20 0 DB, RHO= .8, FSC= .135 HZ, MTIMES= 1, LGMAX=13, KM=110

X THRHLD -3 DB , UNTETHRD, DELT= 074074 SEC, MAX. ABORTS= 20 00 , AT THESEP= 1.00 DEG
PMLS1, BMLS=1 00, S/N= 20 0 DB, RHO= .8, FSC= .135 HZ, MTIMES= 1, LGMAX=13, KM=110

Fig. 6.15

RMS Error Studies; High S/N, Heavy Interference

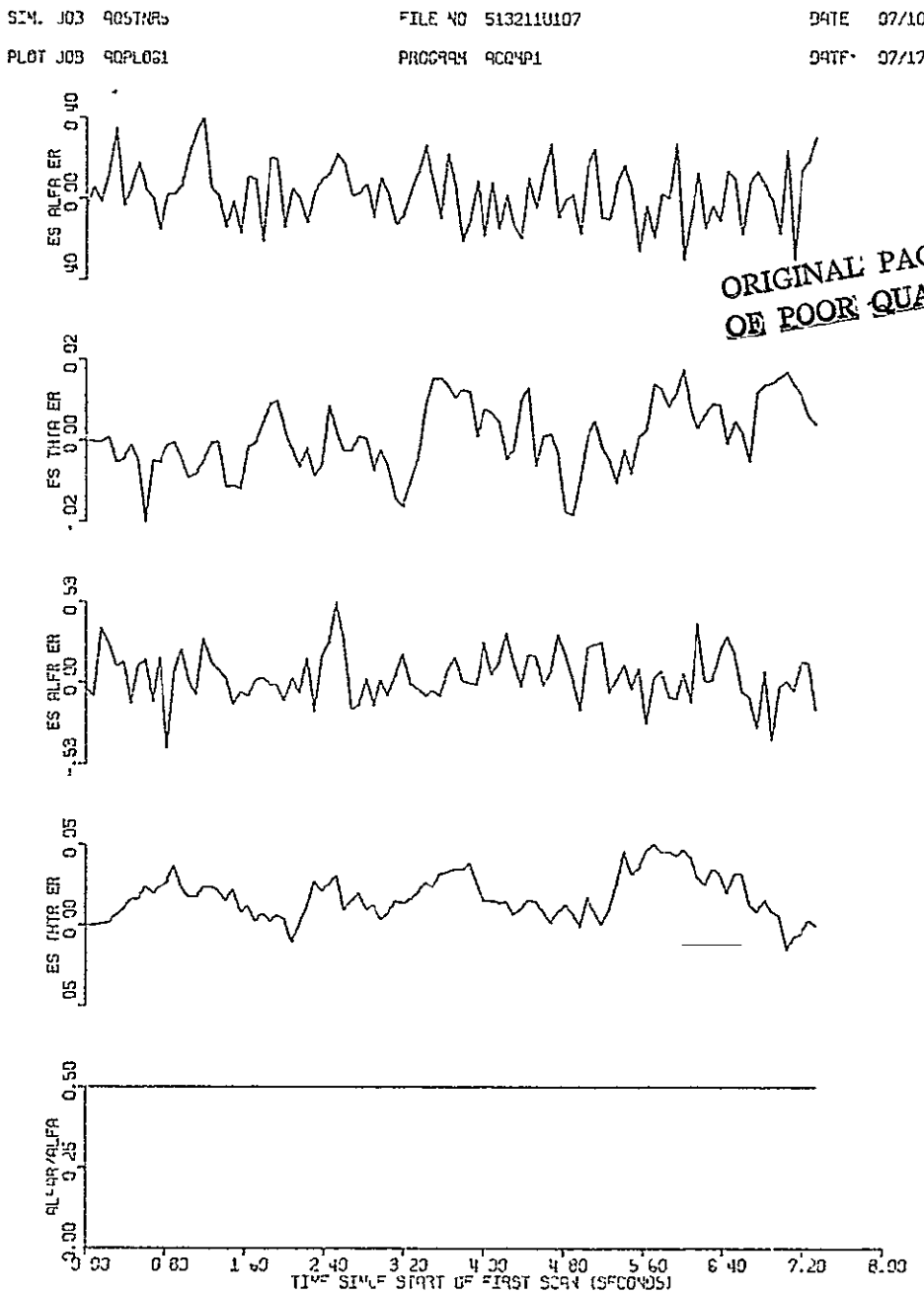

SCENARIO ACQSITNL, PNLS1, BWLS= 1 0 DEG, DELT= 0740741 SEC, KM=100, KSTART= 1
S/N 20 0 DB, RHO= 5, BETA= 15 0 DEG,FSC=, 0 000 HZ, THESEP= 1 880 DEG
RECEIVER SUBOPT, ADAPTIV, UNIFORM, PORTI, BRCVR 1 0 DTG

Fig. 6.16

Acquisition Scenario.
Reference Case: Steady-State Tracking; θ_{sep} = 1.88°

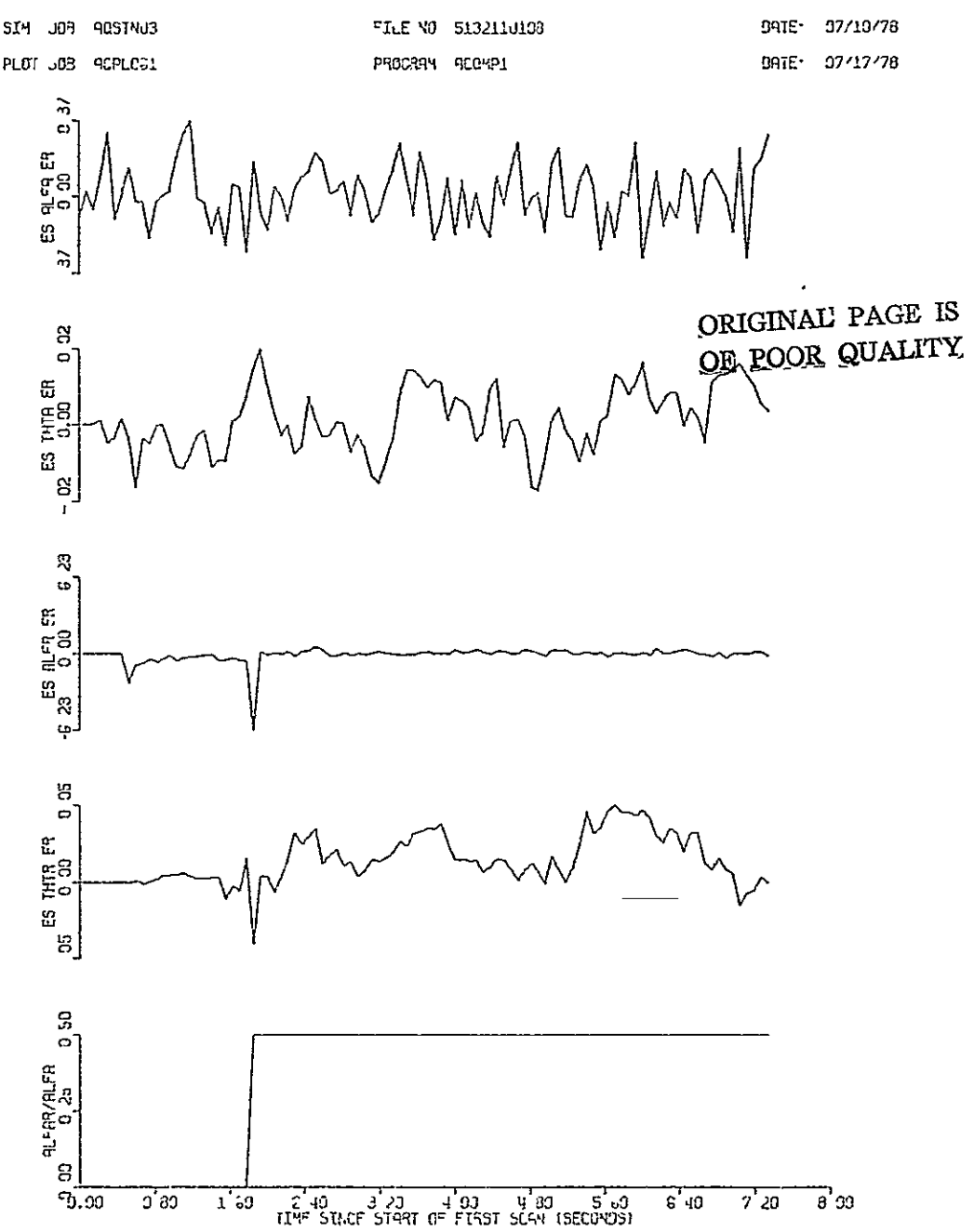

SCENARIO 9QQSIN1, PULSE, SNLS= 1 0 DTG, DELT= 0740741 SEC, KN=100, KSTART= 36
S/N= 20 0 DB, SNO= .5, BETA= 45 0 DEG,FSC=, 0 000 HZ, THESEP= 1 000 DEG
RECEIVER: SUBOPT, ADAPTIV, UNTETHRD, PORT1, DRIVR= 1 0 DEG

Fig. 6.17

Acquisition Scenario.
Interference Acquisition when Initial θ_R Error = 0° and θ_{sep} = 1.88°

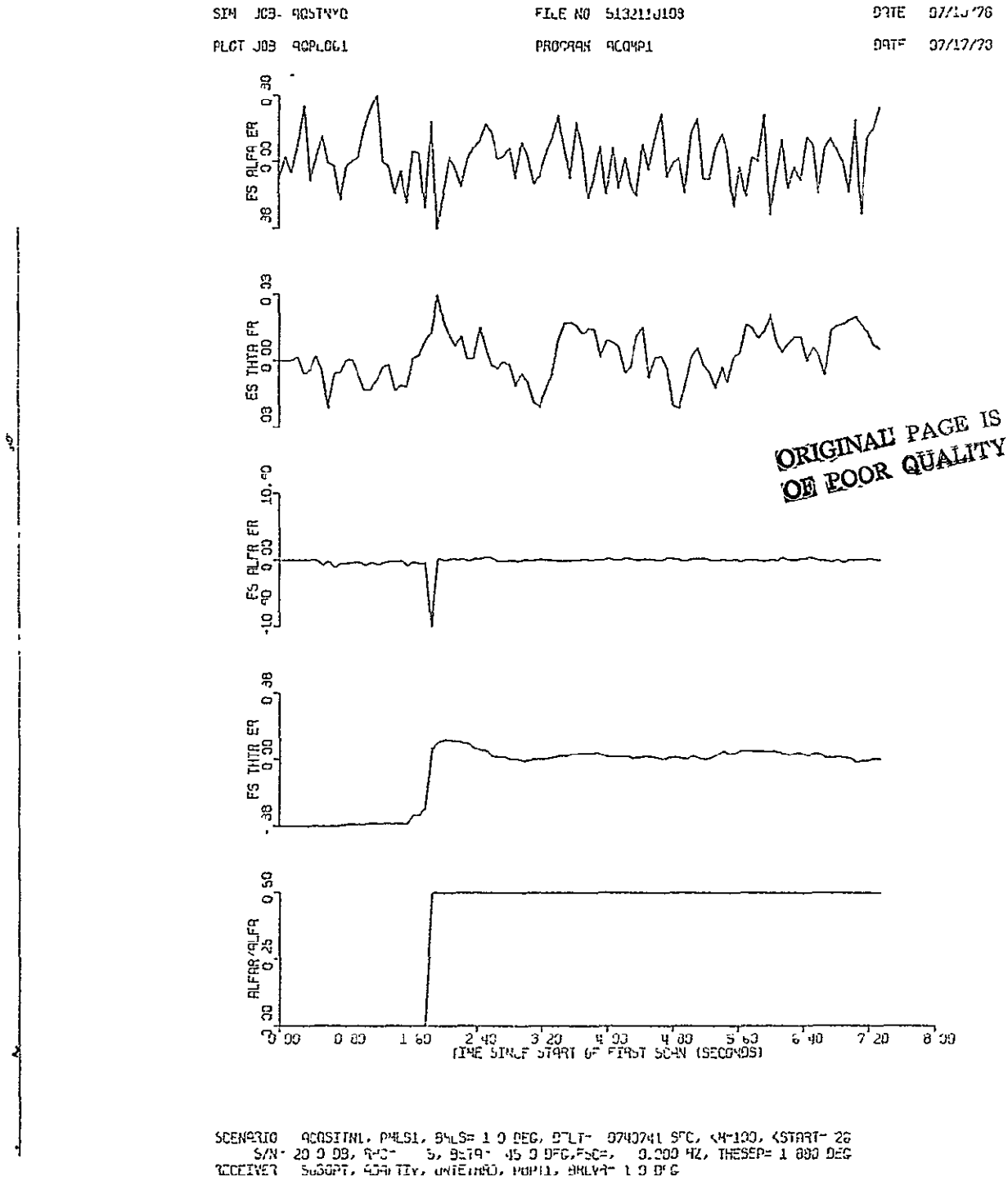

Fig. 6.18

Acquisition Scenario.
Interference Acquisition when Initial θ_R Error = 0.38° and θ_{sep} = 1.88°

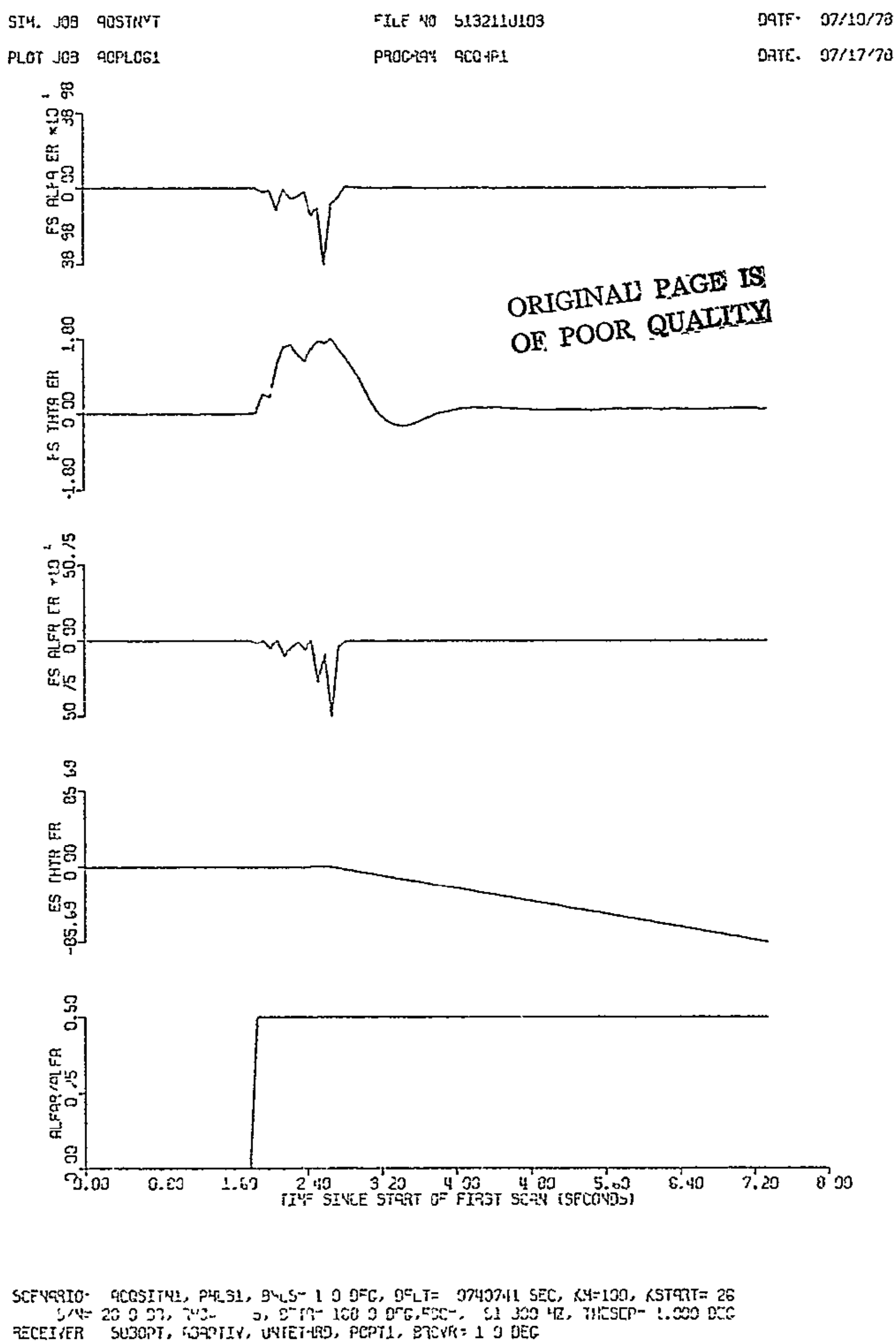

Fig. 6.19

Acquisition Scenario.
Unsuccessful Interference Acquisition when $\theta_{sep} = 1.0°$

after the 26th scan, as in Fig. 6.16. It showed that the suboptimal receiver acquired the multipath signal successfully from an initial error of 0°. Figure 6.18 shows another successful acquisition for $\theta_{sep} = 1.0°$, even when the initial θ_R error is -0.38°. Fig. 6.19 shows an acquisition failure attributable to the reduction of θ_{sep} in this run to 1.0°. The loss of acquisition capability with diminishing separation angle is believed to be related to the steady-state tracking difficulty noted in the RMS error studies above. Solution of the acquisition problem should accompany the solution of the prior problem.

CHAPTER 7

CONCLUSION

Previous results had shown that the optimal receiver was generally superior to the threshold receiver by a factor of about 20:1; however, its complexity was a distinct disadvantage. The order of the state vector and the inclusion of in the state vector caused an acquisition problem. The objective in developing the suboptimal receiver was to reduce the complexity of the algorithm in exchange for an acceptable decrease in performance.

The results obtained in this study can be summarized in three sections.

Crossing Multipath Study

The integrated LOE/Kalman filter suboptimal receiver algorithm tested in simulation was generally superior to the threshold receiver but, as expected, inferior to the optimal receiver. The reduction of the order of state vector and parameter vector simplified the structure of the receiver itself. The employment of the table lookup technique did speed up the computation required in the suboptimal receiver; however, the length of the computation time still limited the capability of the suboptimal receiver, because we used a general-purpose minicomputer. By adequate usage of special-purpose microprocessors or good approximation functions, this problem may be eliminated.

RMS Error Study

Difficulties in steady-state tracking were noted that appear to be analogous to the difficulties in resolving two closely spaced radar targets with a finite aperture antenna. "To resolve, or not" is a question that needs to be answered (dynamically, as a function of θ_{sep}) in the MLS receiver problem, and an answer in the negative cannot be immediately ruled out as second best in this case. The problem is being studied.

Acquisition Scenario Study

The difficulty in acquiring β was solved by averaging β out of the parameter vector in the suboptimal receiver. The simulation study revealed both success and failure in acquisition. A more thorough study of the acquisition problem is in progress to establish that the suboptimal receiver can acquire when it can track.

REFERENCES

1. McAlpine, G. A., Highfill, J. H., III, Irwin, S. H., & Padgett, J. E., "Optimization of MLS Receivers for Multipath Environments,' Rpt. #EE-4033-101-75, Research Laboratories for the Engineering Sciences, School of Engineering and Applied Science, University of Virginia, Charlottesville, Virginia, 22901, Dec. 1975.

2. McAlpine, G. A., Highfill, J. H., III, Irwin, S. H., Nelson, R. E., & Koleyni, G., "Optimization of MLS Receivers for Multipath Environments," Rpt. #UVA/528062/EE77/104, Research Laboratories for the Engineering Sciences, School of Engineering and Applied Science, University of Virginia, Charlottesville, Virginia, 22901, Nov. 1977.

3. McAlpine, G. A., Highfill, J. H., III, & Irwin, S. H., "Optimization of MLS Receivers for Multipath Environments," Rpt. #EE-4633-102-76, Research Laboratories for the Engineering Sciences, School of Engineering and Applied Science, University of Virginia, Charlottesville, Virginia, 22901, Mar. 1976.

4. McAlpine, G. A., Highfill, J. H., III, & Irwin, S. H., "Optimization of MLS Receivers for Multipath Environments, Rpt. #UVA/528062/EE76/103, Research Laboratories for the Engineering Sciences, School of Engineering and Applied Science, University of Virginia, Charlottesville, Virginia, 22901, Dec. 1976.

5. Murphy, James T., Jr., "Locally Optimum Estimation with Applications to Communication Theory," Ph.D. Dissert., Univ. of Florida, 1968.

6. Kelley, R. J., Navigation: Journal of the Institute of Navigation, Vol. 23, No. 1, Spring 1976.

7. "Microwave Landing System," Final Rpt. of the Scanning Beam Working Grp., prepared for Dept. of Transp., Fed. Aviation Admin., Dec. 1974.

DISTRIBUTION LIST

Copy No.

1 - 2 NASA Scientific & Technical Information Facility
PO Box 8757
Baltimore/Washington International Airport
Baltimore, MD 21240

3 - 13 Flight Electronics Division
National Aeronautics and Space Administration
Langley Research Center
Hampton, VA 23365

attn: Mr. W. T. Bundick
Technical Officer

14 - 15 G. A. McAlpine

16 - 20 J. H. Highfill III

21 C.-P. J. Tzeng
International House, 822
University of California
Berkeley, CA 94720

22 Ghassem Koleyni

23 E. A. Parrish, Jr.

24 I. A. Fischer

25 - 26 E. H. Pancake
Science/Technology Information Center
Clark Hall

27 RLES Files

9536:mjq

UNIVERSITY OF VIRGINIA

School of Engineering and Applied Science

The University of Virginia's School of Engineering and Applied Science has an undergraduate enrollment of approximately 1,000 students with a graduate enrollment of 350. There are approximately 120 faculty members, a majority of whom conduct research in addition to teaching

Research is an integral part of the educational program and interests parallel academic specialties These range from the classical engineering departments of Chemical, Civil, Electrical, and Mechanical to departments of Biomedical Engineering, Engineering Science and Systems, Materials Science, Nuclear Engineering, and Applied Mathematics and Computer Science In addition to these departments, there are interdepartmental groups in the areas of Automatic Controls and Applied Mechanics All departments offer the doctorate; the Biomedical and Materials Science Departments grant only graduate degrees

The School of Engineering and Applied Science is an integral part of the University (approximately 1,400 full-time faculty with a total enrollment of about 14,000 full-time students), which also has professional schools of Architecture, Law, Medicine, Commerce, and Business Administration. In addition, the College of Arts and Sciences houses departments of Mathematics, Physics, Chemistry and others relevant to the engineering research program. This University community provides opportunities for interdisciplinary work in pursuit of the basic goals of education, research, and public service.